IPS Meeting 2014
26 - 28 February

Institute of Physics Singapore

Conference Program

The IPS Meeting 2014 thanks its sponsors
for their generous support

Institutional Sponsors:

1 Foreword

Dear fellow Physicists,

this year 2014, the IPS meeting is riding over again to the shores of the National University of Singapore for our annual gathering together between physicists active in research. The facilities at the newly built University Town should provide a nice environment for a relaxed exchange with colleagues you may not know that they are active in Singapore.

This year saw a strong development in our research community on topological insulators, and we have two new sessions dedicated to that. There were exciting developments with cloaking techniques, and we are lucky to have Baile Zhang from NTU, one of the experimental stars in that field, giving us an update in a plenary lecture. Similarly, we are lucky to have Jose Ignacio Latorre from Barcelona with us, who should be able to explain to all those of us who don't really want to admit to not have understood the ideas behind the Higgs particle, which cashed in this year's Nobel prize in physics.

With over 70 talks, over 20 of them invited, and over 50 poster presentations, we really are a strong local community. Most of our participants still come from the universities. So if you have a colleague who is maybe a bit shy in showcasing what research they do, encourage them to take part in this annual event, and get connected again with the next generation of researchers!

As usual, we tried to find a balance between bringing people together with similar interest, and encourage exchange between different fields with the composition of the 18 different technical sessions. The location ensures that you are never far away from the other session if you want to sneak into something completely different.

Posters are always a very relaxing and scientifically stimulating way of communication. The poster pitch pitch competition we tried last year seemed to work fine, where poster presenters can give you a 3-minute advertiser for their work. We have it again this year, together with ample of time to hang around posters, or catch up with the exhibitors who not only provide you with research equipment and services, but have often research experience as well. Since discussing exciting science drains a lot of energy, and also because it is a lot more fun, the long poster session on Thursday evening comes with food again. Just hang around and see what is going on, and take the opportunity to ask your colleagues questions in a relaxed atmosphere.

Again, the organization of this meeting had strong support from NTU, NUS, and IHPC. Big thanks to our logistics support team with Andreas Dewanto, Evon Tan, the team

from University Town facility management, and many physics students NUS and CQT.

We are also happy again to acknowledge our institutional supporters, the Department of Physics at NUS and the School of Physics and Applied Physics at NTU, as well as the Centre for Quantum Technologies. Last but not least, let's thank our exhibitors, who again help with their generous sponsorship to make this conference possible.

With this, we wish you a stimulating conference, with a lot of new ideas, contacts and collaborations for a successful year of research in physical sciences ahead!

Your organizing team of the IPS meeting 2014

Contents

2 Schedule

Wednesday, 26 February

8.45 AM	Registration		
9.30 AM 9.45 AM	Opening Address (auditorium) Plenary talk 1: Claus-Dieter Ohl (auditorium)		
10.30 AM	Coffee/Tea Break + Exhibition + Poster mounting		
11.00 AM	Plenary talk 2: Zhang Baile (auditorium)		
11.45 AM	Exhibition + Poster mounting		
12.30 PM	Lunch + Posters + Exhibition		
1.30 PM	Technical Sessions		
	T1 (Room 1+2) Twodimensional Materials	T2 (Room 3+4) Bubbles and Cavitation	T3 (Room 5+6) Quantum Information 1
3.00 PM	Coffee/Tea Break + Exhibition		
3.30 PM	Technical Sessions		
	T4 (Room 1+2) Plasma PhysicsTopological Insulators 1	T5 (Room 3+4) Topological Insulators 1	T6 (Room 5+6) Quantum Information 2
5.00 PM	End of Wednesday sessions		

Thursday, 27 February

9.00 PM	Registration		
9.30 AM 10.15 AM	Plenary talk 3: Jose Ignacio Latorre (auditorium) Plenary talk 4: Sow Chorng Haur (auditorium)		
11.00 AM	Coffee/Tea Break + Exhibition + Poster mounting		
11.30 AM	PO1: Poster Pitch session		
12.30 PM	Lunch + Posters + Exhibition		
1.30 PM	Technical Sessions		
	T7 (Room 1+2) Topological Insulators 2	T8 (Room 3+4) Lasers	T9 (Room 5+6) Atomic and Molecular Physics
3.00 PM	Coffee/Tea Break + Exhibition		
3.30 PM	Technical Sessions		
	T10 (Room 1+2) Plasmonics and Metamaterials	T11 (Room 3+4) Nonlinear Optical Phenomena	T12 (Room 5+6) Atom-Photon Interaction
5.00 PM	PO2: Pizza + Poster + Exhibition		
6.37 PM ($+\epsilon$)	Poster awards		
7.00 PM ($+\epsilon'$)	End of Thursday sessions		

Friday, 28 February

9.00 AM	Technical Sessions			
	T13 (auditorium) Oxide Materials	T14 (Room 1+2) Soft Condensed Matter	T15 (Room 3+4) Ultrafast Spectroscopy	T16 (Room 5+6) Quantum Sensing
10.30 AM	Coffee/Tea Break + Exhibition			
11.00 AM	Technical Sessions			
	T17 (auditorium) Materials for Energy Conversion	T18 (Room 1+2) Physics of Batteries	T19 (Room 3+4) Special Topics	
12.30 PM	End of Friday sessions			

3 Location Map

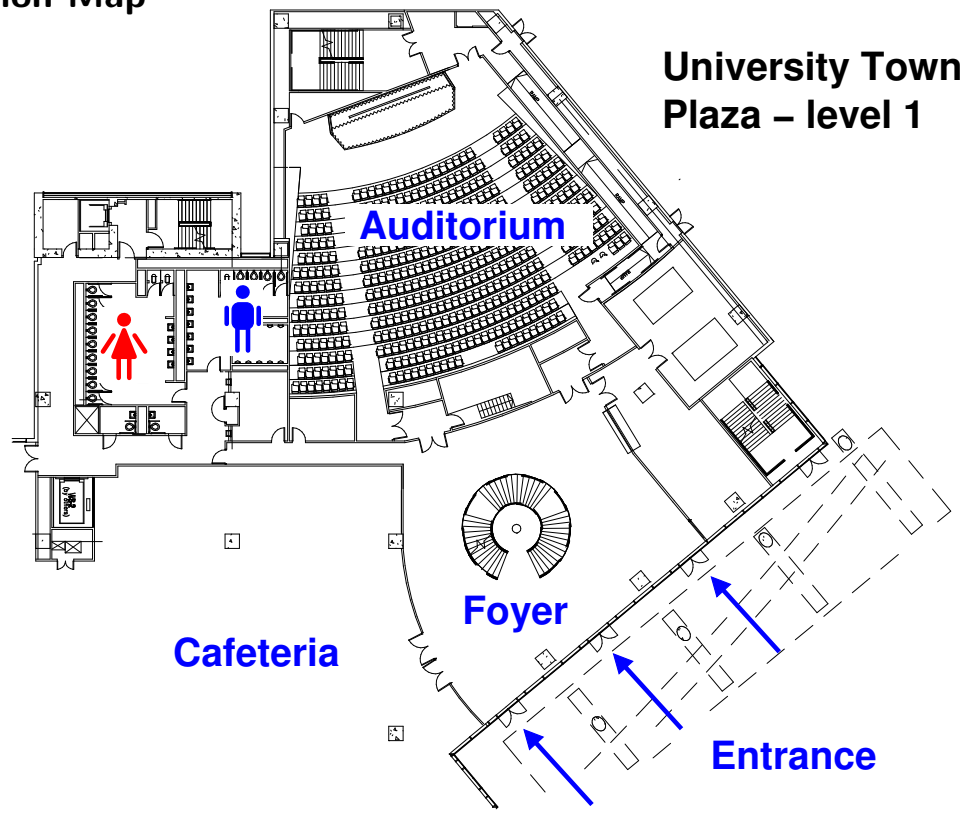

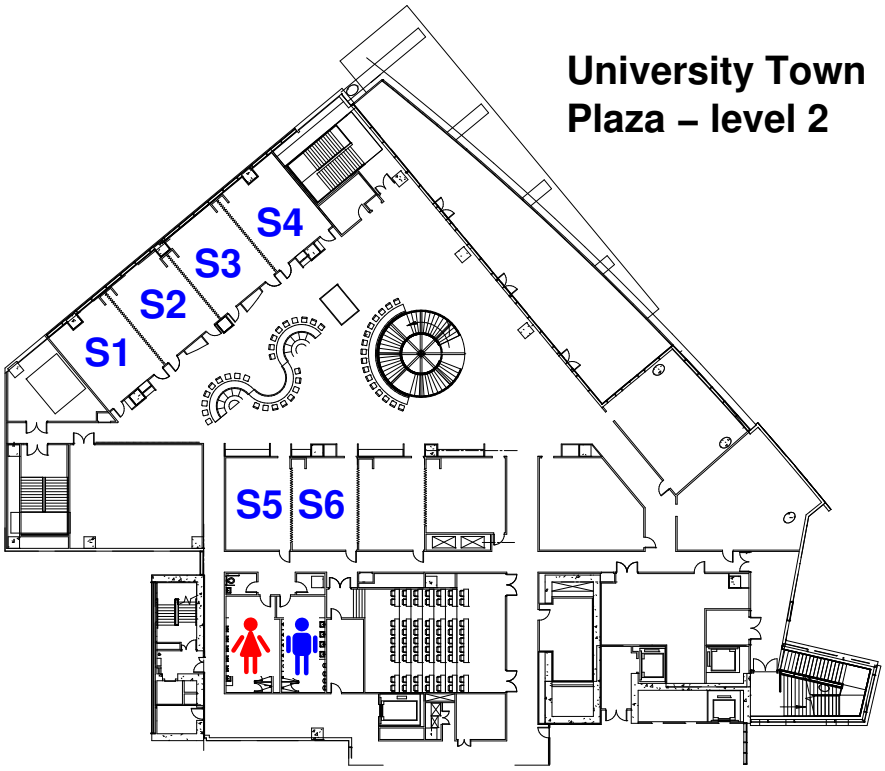

4 Plenary sessions

We will have four distinguished plenary speakers from near and far this year – the topics are very diverse, but also accessible for every Physics researcher!

4.1 Claus-Dieter Ohl: Surface Nanobubble Dynamics

Wednesday, 26 February, 9:45am

Abstract

In the last 10 years convincing evidence has been gained that surfaces submerged in liquids supersaturated with gas stabilize nanometer sized bubbles. They are a curiosity as standard thermodynamic theory predicts that nanobubbles should dissolve within milliseconds, yet they remain stable for days. Besides this unsolved scientific curiosity, they are very important for industrial applications: In liquid flows, surfaces determine as boundaries the flow field above. If surfaces as partly covered with gas they strongly increase slip and thereby reduce skin friction. This may have important consequences for membrane filtering transport of flows within porous media/rocks. Besides nanobubbles are optical elements and must at all cost be avoided in IC fabrication processes.

In this talk I'll summarize the current research in our group on nanobubble studies using transmission electron, optical, and atomic force microscopy. We'll demonstrate the first dynamic measurements of nanobubble response to forces and coalescence events. Although we have proven that some theories explaining their stability are wrong we have not yet a good answer either.

About the Speaker

Claus-Dieter Ohl has studied Physics in the University of Darmstadt (1994) and the University of Goettingen (PhD 1999), Germany. After postdoc stints at Johns Hopkins and the University of Twente he joined NTU as a faculty member in 2007. His research interests are classical fluid dynamics, acoustics, biological applications, micro and nanofluidics.

He also holds an adjunct position with the A*Star Institute for High performance Computing (IHPC).

4.2 Zhang Baile: Confusions, Solutions, and Prospects in Invisibility Cloaking Research

Wednesday, 26 February, 11:00am

Abstract

There is hardly a research topic in history that could stir up so much enthusiasm in the scientific community and, at the same time, lots of aversion on the other hand, as did invisibility cloaking. Whether it is a real revolution towards the long-cherished dream, or merely a blue-sky physics hype that cannot last for long, still lacks a clear conclusion. In this talk, I will talk about a number of typical confusions, some of which have caused intense discussions in the past few years, and their solutions regarding invisibility cloaking. The prospects of invisibility cloaking will also be discussed from my viewpoint.

About the Speaker

Dr. Baile ZHANG is currently an assistant professor in the School of Physical and Mathematical Sciences at Nanyang Technological University, Singapore. He was a postdoctoral associate in the biological group "BioSyM" at Singapore-MIT Alliance for Research and Technology Centre from 2009 to 2011. He received his Ph.D. in 2009 from MIT, following his B.S. degree in 2003 and M. S. degree in 2006 from Tsinghua University in Beijing, all majored in Electrical Engineering. His current research interests include electromagnetic wave theory and applications, metamaterials, optical microscopy, and photonics. He is a recipient of MIT Technology Review TR35 Global Young Innovators Award of 2012. He was invited to give a TED Talk at TED2013 Conference in Long Beach, California, as the first Chinese TED Fellow. He serves on the Editorial Board of Scientific Reports.

4.3 José Ignacio Latorre: The Higgs in simple words

Thursday, 27 February, 9:30am

Abstract

We give a non-technical presentation of the world of elementary particles and the need for a final ingredient: the Higgs boson. This particle was predicted in 1964 but all experiments to detect it failed for four decades. A collective effort to construct the Large Hadron Collider at CERN has finally succeded to find the Higgs particle. This is a wonderful story about intelligent human collaboration and the universality of Science.

About the Speaker

Prof Jos/'e I. Latorre got a Ph.D. in High Energy Physics, and worked as postdoc at MIT and at the Niels Bohr Institute in Copenhagen. He is the director of the Center for Scientific Research at Benasque. His interests also include research in the field of Quantum Information, as well as scientific outreach and business innovation. He also co-created a research team that delivers a tool used to compute all the processes observed at the LHC, located at CERN.

4.4 Sow Chorng Haur: Introducing Interactive Demonstrations in Science Teaching

Thursday, 27 February, 10:15am

Abstract

Science demonstrations are valuable as they provide exciting, visually appealing and thought provoking stimuli to promote a culture of inquiry and interactive teacher-student exchanges in the classroom. The demonstrations add reality and vividness in the process of concept formation as a visual aid, and/or showing an example of the application of a principle. Some concepts are best illustrated using demonstrations, which also help to address misconceptions. Demonstrations can form a key part of a student's classroom experience provided they are integrated with and supported by effective pedagogical theory so that they are carried out in a way that facilitates learning. Traditionally-presented demonstrations, in which students are passive audience watching the demonstration and hearing the teacher's explanation, may not effectively help students grasp the underlying scientific concepts or spot and correct misconceptions. The key is to vary the mode of presentation of the demonstration and design classroom activities to go along with the science demonstrations with the aim to maximize active participation and engagement of the students. In this presentation, we will share our experience in the development of the NUS FoS Science Demo Lab and some of the strategies we have attempted in the presentation of the science demo.

About the Speaker

Chornghaur Sow received the B.Sc. (first-class honors) and M.S. degrees in physics from the National University of Singapore (NUS), Singapore, in 1991 and 1993, respectively, and the Ph.D. degree from the University of Chicago in 1998. During 1999-2000, he was a Postdoctoral Fellow with Bell Labs, Lucent Technologies. He has been with the Department of Physics, Faculty of Science, NUS, since 2001, where he is currently an Associate Professor. He has authored or coauthored a number of papers in the field of nanoscience and nanomaterials. In teaching, he is the founding member of the Faculty of Science -Science Demonstration Laboratory and has been developing the teaching approach of using Science Demonstration in enhancing students' learning. He is currently a Fellow of the NUS Teaching Academy.

5 Posters

5.1 Poster pitch student competition - Session PO1 (Thursday)

We felt the last year's trial with the poster pitch mini-presentations worked out well, so we continue it. Again a full session (PO1, Thursday before lunch) with no parallel technical sessions where all IPS participants get your audience for a supershort (3 minutes) presentation on a poster if the authors want to participate. In order to encourage authors to participate, we will choose the Best Poster Award this year form those submissions where there was short presentation in this session PO1.

For this, we just project your poster on the screen in the lecture hall (please provide us with a PDF file for that purpose). You can email this to us via postersipsmeeting.org, or leave it with the reception desk.

IPS Best Poster Award

During the conference the program committee will select the three best poster presentations for the IPS Best Poster Award. The award will be handed over to the winners at the Poster & Pizza session PO2 on Thursday evening, probably around 6pm-7pm at (Location TBA).

Logistics

Timing

Posters are presented during the whole conference; perhaps you can make sure that the posters are up as soon as you can. We encourage everyone to browse around during coffe breaks and lunchtime (catered lunch is nearby). We would recommend that the best time for the poster presenters to be around at the poster is the Thursday evening session that comes together with some Pizza as well. Please take down the posters by latest at the end of the conference, i.e., on Friday noon latest.

Location

The main poster area will be in the level 2 of the Utown Plaza. Each poster is assigned a panel which corresponds to the number listed below, e.g., the panel no. 23 is reserved for P23 and so on. We will provide Velcro strips to mount the posters on the wall, please see the reception desk for this.

Format

We have been told that the poster walls are just a little too small for A0 posters. To play safe, we recommend to use a A1 portrait poster format.

5.2 Poster Session (Thursday)

Below, we show a list of abstracts submitted by the authors. We provide a panel number so you can locate the poster of your interest better, and also the easychair number from the poster submission.

P1 Demonstration of genuine multipartite entanglement with device-independent witnesses

Julio Barreiro, Jean-Daniel Bancal, Philipp Schindler, Daniel Nigg, Markus Hennrich, Tomas Monz, Nicolas Gisin, Rainer Blatt

Thursday 05.00 PM, Foyer/Hallway, Panel 1 (EC number: 1)

Entanglement in a quantum system can be demonstrated experimentally by performing the measurements prescribed by an appropriate entanglement witness. However, the unavoidable mismatch between the implementation of measurements in practical devices and their precise theoretical modelling generally results in the undesired possibility of false-positive entanglement detection. Such scenarios can be avoided by using the recently developed device-independent entanglement witnesses (DIEWs) for genuine multipartite entanglement. Similarly to Bell inequalities, DIEWs only assume that consistent measurements are performed locally on each subsystem. No precise description of the measurement devices is required. Here we report an experimental test of DIEWs on up to six entangled 40 Ca^+ ions. We also demonstrate genuine multipartite quantum nonlocality between up to six parties with the detection loophole closed.

P2 Spin-dependent electron transport in a Rashba quantum wire: effects of the edge disorder

Xianbo Xiao

Thursday 05.00 PM, Foyer/Hallway, Panel 2 (EC number: 4)

We investigate theoretically the spin-dependent electron transport in a Rashba quantum wire with rough edges. The charge and spin conductances are calculated as function of the electron energy and wire length by adopting the spin-resolved lattice Green function method. For a single disordered Rashba wire, it is found that the charge conductance quantization is destroyed by the edge disorder. However, a nonzero spin conductance can be generated and its amplitude can be manipulated by varying the wire length, which is attributed to the broken structure symmetries and the spin-dependent quantum interference induced by the rough boundaries. For a large ensemble of disordered Rashba wires, the average charge conductance decreases monotonically, however, the average spin conductance increases to a maximum value and then decreases, with increasing wire length. Further study shows that the influence of the rough edges on the charge and spin conductances can be eliminated by applying a perpendicular magnetic field to the wire. In addition, a very large magnitude of the spin conductance can be achieved when the electron energy lies between the two thresholds of each pair of subbands. These findings

may not only benefit to further apprehend the transport properties of the Rashba low-dimensional systems but also provide some theoretical instructions to the application of spintronics devices.

P3 Nuclear Octupole Moment Measurement of $^{137}Ba^{+}$ Ion

Nick Lewty, Murray Barrett

Thursday 05.00 PM, Foyer/Hallway, Panel 3 (EC number: 5)

We perform precision measurements on the $5D_{5/2}$ manifold hyperfine intervals of a single trapped ion, $^{137}Ba^{+}$. RF spectroscopy is used to measure the hyperfine intervals to an accuracy of a few Hz. Our results provide a three orders of magnitude improvement in accuracy over previous work and also provide a 10-fold improvement in the value of g_J for this level. These results complement our previous work on the $5D_{3/2}$ manifold of $^{137}Ba^{+}$, providing an independent measurement of the nuclear octupole, and a consistency check on atomic structure calculations.

P4 N-doped graphene wrapped micro-sized Si film as anodes for lithium-ion batteries with industrial-level initial coulombic efficiency

Dongliang Chao, Zexiang Shen

Thursday 05.00 PM, Foyer/Hallway, Panel 4 (EC number: 12)

A high initial coulombic efficiency (ICE) and stable Si-based anode for lithium-ion batteries (LIB) is critical for energy storage. Here we report a new type of freestanding LIB anode composed of micro-sized Si particles wrapped by nitrogen-doped graphene (mSi@NG) film by a rapid, one-step freeze-drying route. This is the first report on using graphene as the binder/current collector in the synthesis of mSi-based anode for LIB; the electrochemical tests and Raman spectra analyses prove that the N-doping graphene could effectively improve the overall electrochemical performance of mSi anode, especially for the ICE property: 85% which make the industrial application of mSi possible. It is also proved for the first time that graphene can carry and control solid electrolyte interphase (SEI) during first discharging process, which can protect mSi from being etched by electrolyte. Thus, the graphene coating can not only improve the electric connectivity of the whole electrode, accommodate the volume expansion of mSi, but also protect the mSi from over-lithiation and fracture via forming a stable SEI prior on graphene layer surfaces. We believe that the synthesis of mSi@NG composite film may provide a low cost, high efficiency, and scalable mass-production method to prepare micro-Si based materials for electrochemical energy storage.

P5 MoS_2-CNTs Hybrid as Photo-Detector

Kah Whye Woo, Junju Ng

Thursday 05.00 PM, Foyer/Hallway, Panel 5 (EC number: 14)

Single-layer Molybdenum disulfide (MoS_2) has many unique properties including its semi-conductance and strong photoluminescence. As such, there is great interest in harnessing its properties for a variety of applications, including photoelectronics and optoelectronics. By assembling single-layer MoS_2 onto Carbon Nanotubes (CNTs), the physical and electrical properties of the MoS_2-CNT composite will be more desirable than the individual components. Here, we report viable physical methods of the assembly of single-layer MoS_2 onto CNT. The assembly was achieved through a dropcast or film method, with the latter resulting in thin layer MoS_2 on top of CNTs. The presence of MoS_2 was verified using Raman Spectroscopy and visual images from optical microscope and scanning electron microscope (SEM) imaging. The MoS_2-CNT composite was found to have an increase in photocurrent when exposed to external excitation by a broad beam of laser hence, making it possible for the hybrid system to serve as a photo detector.

P6 Carbon Nanotubes Actuators: A Fundamental Study

Kai Song, Xin Yi Kendra Chan

Thursday 05.00 PM, Foyer/Hallway, Panel 6 (EC number: 16)

Carbon Nanotubes (CNTs) actuation has been demonstrated on individual CNTs, CNT sheets and CNT/polymer composites. Work done by others suggests that the actuation is due to a laser induced electrostatic interaction mechanism. This work aims to establish a scientific study on the electrostatic interaction by coating insulator hafnium(IV) oxide (HfO2) and gold (Au) on As-Grown CNT samples.

CNTs are synthesized using a Plasma Enhanced Chemical Vapor Deposition (PECVD). Actuators are cut using an Optical Microscope Focused Laser Beam Set-up. Length, width, trench width at left and right side of actuators and the power of laser shining on the actuator are the parameters affecting the magnitude of actuation.

A searching of the optimum parameters is carried out by varying one parameter at a time while keeping the other parameters constant. Images of actuator with and without laser shining on it are taken and the displacements are measure using computer software ImageJ.

Samples with both top and side coatings are prepared by cutting the actuators with optimum parameter before coating of materials. Samples with only top coating are prepared by coating the materials followed by cutting of actuators. Characterisation of the coated materials is performed using Scanning Electron Microscope (SEM) and Energy-Dispersive X-ray Spectroscopy (EDX).

Actuations of actuators on coated samples are measured. A preliminary study on the results has been suggestive and the comparison allows us draw interesting conclusions on the mechanism of CNT actuation. The heating effect of the laser also presumably affects the coating and hence CNT actuation.

P7 Giant Magnetocaloric Effect in Magnetoelectric $Eu_{1-x}Ba_xTiO_3$

Km Rubi, Pawan Kumar, Mahendiran Ramanathan

Thursday 05.00 PM, Foyer/Hallway, Panel 7 (EC number: 19)

We report magnetization and magnetic entropy change (Sm) in magnetoelectric $Eu_{1-x}Ba_xTiO_3$ for $0.1 \leq x \leq 0.9$. The divalent Eu (S = 7/2) orders antiferromagnetically below TN = 4.5 K in $x = 0.1$ and TN most likely shifts to lower temperature for higher x. All the compounds show field-induced paramagnetic to ferromagnetic transition over a finite temperature range above TN. We find $S_m = 40$ J/kg.K for H = 5 T at TN in x = 0.1, which is the largest value among Eu-based oxides and chalcogenides. While Sm decreases with increasing x, the observed value of $S_m = 7$ J/kg.K even in the most spin diluted composition $x = 0.9$ is much larger than values found in many ferromagnetic manganites. Our results indicate that these compounds will be of interest for cryogenic magnetic refrigeration.

P8 Magnetoresistance and magneto Thermopower of $Nd_{1-x}Sr_xCoO_3$ series.

Pawan Kumar, Ramanathan Mahendiran

Thursday 05.00 PM, Foyer/Hallway, Panel 8 (EC number: 21)

We studied electrical, magnetic and thermal properties of $Nd_{1-x}Sr_xCoO_3$. A rapid increase in TC with Sr doping and an anomalous peak at a temperature $T* \ll TC$ occurs in magnetization, which also shifted to higher temperature with Sr doping. Up to $x = 0.2$ doping system stays in semiconducting state throughout temperature range and for $x = 0.3$ and above doping system goes to metallic state.Thermopower stays positive for lower doping ($x \leq 0.3$) until low low temperature and changes sign for higher doping ($x \geq 0.4$) with temperature. Thermopower for semiconductor samples goes through a maximum which was attributed to change in the resistivity characteristic behaviour from variable range hopping to thermally activated conduction. For metallic samples ($x = 0.3, 0.4$) also goes through a maximum which is also attributed to characteristic of TEP in two different state (ferromagnetic and paramagnetic). The Magnetoresistance and Magneto thermopower also have been studied on some specific samples. Large magneto thermopower (35% for $x = 0.4$) compare to Magneto Resistance (4%) has been found.

P9 EIT-based light storage using metastable helium hot vapor

Musawwadah Mukhtar

Thursday 05.00 PM, Foyer/Hallway, Panel 9 (EC number: 23)

In this work, we present light storage based on electromagnetically induced transparency (EIT) using metastable helium vapor in room temperature. Absorption of medium is eliminated in presence of a strong control beam. In addition, it exhibits steep refractive index variation, which gives slow-light effect; the group velocity of light can be reduced to 5 km/s. In EIT-based storage, a light pulse can be turned onto atomic excitation (Raman coherence) and be reverted by switching off and on the control beam. This system can achieve 11% efficiency for a 3 μs storage time. In particular, we did study

of light storage with optically detuned light; the detuning ranges between 0 and 2 GHz, twice the Doppler linewidth. This is possible thanks to the absence of hyperfine structure. Our work could have application for quantum information processes. Besides, light soliton and atomic excitation involved in our system can be thought as pseudo-particle, so-called dark-state polariton. Based on works on means to enhance nonlinearity in EIT, we will discuss the possibility of studying many-body quantum physics with light.

P10 Giant magnetothermopower in charge ordered $Nd_{0.75}Na_{0.25}MnO_3$

Durga Venkata Maheswar Repaka, Mahendiran Ramanathan

Thursday 05.00 PM, Foyer/Hallway, Panel 10 (EC number: 25)

We report magnetization, resistivity and thermopower in the charge-orbital ordered antiferromagnet $Nd_{0.75}Na_{0.25}MnO_3$. Magnetic-field induced collapse of antiferromagnetism is found to be accompanied by a giant negative magnetothermopower (= 80-100% for a field change of 5 T) over a wide temperature (T = 60-225 K) and giant magnetoresistance. While the field-induced metamagnetic transition in magnetization is reversible upon field-cycling at T >40 K, it is irreversible at lower temperatures and this has impact on magnetoresistance, magnetothermopower as well as change in the temperature of the sample. Our results indicate high sensitivity of thermopower to changes in the magnetic state of the sample.

P11 Molten Salt Synthesis and Characterization of K2(M2Sn6)O16 (M = In, Co) and its Anodic Studies

Tran Thuy Linh, Dang Thu Hien, M V Reddy, Stefan Adams, B V R Chowdari

Thursday 05.00 PM, Foyer/Hallway, Panel 11 (EC number: 26)

Nano/submicronsized K2(M2Sn6)O16 (M = In, Co) compounds were prepared and investigate their properties as an anode material in Li-ion batteries. Nano-K2(M2Sn6)O16 (M = In, Co) were synthesized by molten salt method (MSM) using KCl at 850°C, or KCl/NaCl at 650°C for 3h in air. The compounds were characterized by Rietveld refined X-Ray Diffraction (XRD), Scanning Electron Microscopy (SEM), Density and Brunauer-Emmett-Teller (BET) surface area methods. All phases exhibited surface areas ranging from 1.31 to 5.68 m^2g^{-1}, densities varying from 7.6730 to 8.8220 gm cm^{-3}. The Li-cycling behavior of M = Co (nano-(K-Co)) and M = In (nano-(K-In)) were examined by galvanostatic cycling (GC) and cyclic voltammetry (CV) using Li-metal as the counter electrode in the voltage range 0.025-1.0V (or 3.0V). Doctor blade technique was used to fabricate the electrode for Li-cycling studies. All compounds display main cathodic peaks at ∼0.7V and anodic peaks at ∼0.5V based on the CV studies. Anodic properties showed a reversible capacity values in the range 639 – 714 mAh/g in the voltage range, 0.005-1.0 V vs. Li. Nano- K2(M2Sn6)O16 (M = In, Co) made from Co-sulfate generally displayed a high stable capacity with good capacity retention. When cycled to higher cut-off voltage (0.005-3.0V) capacity fading was noted in all compounds due to huge

volume variation conversion reaction of Sn, In. Keywords: K2(M2Sn6)O16 (M = In, Co); Molten salt method; Characterization; Anodes

P12 diffraction limited fabry perot cavity in the near concentric regime

Kadir Durak, Chi Huan Nguyen, Stanislav Straupe, Christian Kurtsiefer

Thursday 05.00 PM, Foyer/Hallway, Panel 12 (EC number: 28)

We designed anaclastic cavity mirrors that simplifies the challenging mode-matching in the near concentric region. The cavity is shown to have diffraction-limited performance even for extremely small mode volume. This is in sharp contrast with the behavior of ordinary cavities with plano-concave mirrors, which demonstrate high level of aberrations significantly increasing the losses in the fundamental mode and exciting the higher order modes. The simulation and experimental results suggest that one needs to get rid of the aberrative losses in order to see cavity QED effects. The suggested anaclastic design overcomes this problem. We estimate the related cavity QED parameters and show that the proposed cavity design allows for strong coupling without a need for high finesse or small cavity volume.

P13 Ion gel gated MoS_2 field effect transistors

Leiqiang Chu, Hennrik Schmidt

Thursday 05.00 PM, Foyer/Hallway, Panel 13 (EC number: 31)

The transport properties of MoS_2 in the low carrier density regime are often dominated by trap states and band edge disorder. High carrier density is needed to access truly metallic conduction in MoS_2. Here we investigate the low temperature conductivity of mechanically exfoliated MoS_2 in the highly metallic regime via ion gel gating. By applying dual gate, Fermi level tunability of the devices is significantly enhanced and exhibits layer dependence which we attribute to the screening effect from the adjacent layer.

P14 Vibrational autodetachment of sulfur hexafluoride anions at long lifetime limit

Sebastian Menk, Swarup Das, Klaus Blaum, Manas Mukherjee

Thursday 05.00 PM, Foyer/Hallway, Panel 14 (EC number: 33)

We present our investigation on vibrational auto detachment of electrons from both vibrationally and rotationally excited hot SF_6^- in cryogenic environment. We use cryogenic electrostatic ion beam trap (EIBT) to study the decay of anions at extremely low residual gas densities of $10^4\,\mathrm{cm}^{-3}$. With The cryogenic trap for fast ion beams(CTF) in Heidelberg we have investigated vibrational auto detachment(VAD)of SF_6^- over almost five orders of magnitude and over times up to 100 ms. We modeled our data using statistical rate theory and electron attachment data as well as recent precision calculation

of vibrational frequencies of the anion. We have been able to measure the adiabatic electron affinity of SF_6 to be (0.91 ± 0.07) eV.

P15 Guanine base stacking in G-quadruplex nucleic acids: Energetic and electron transport properties

Christopher Lech, Alexander Voityuk, Anh Tuan Phan

Thursday 05.00 PM, Foyer/Hallway, Panel 15 (EC number: 34)

We survey the geometries of stacked guanine bases from experimental structures within the Protein Data Bank. Using a variety of MD and QM computational approaches, we investigate the energies and electronic transport properties of commonly observed G-tetrad geometries. We show that the heavily overlapped 5/6-ring geometry is the most energetically favorable and demonstrates superior electron-hole transport properties. The findings present here provide insight into how base stacking geometry affects the formation and higher-order assemblies of G-quadruplexes. Our research also provides a foundation for the rational design of conductive G-wire systems.

P16 Towards a lattice of Rydberg atoms

Jingshan Han, Ruixiang Guo, Thibault Vogt, Wenhui Li

Thursday 05.00 PM, Foyer/Hallway, Panel 16 (EC number: 36)

Rydberg atoms are highly excited atoms, having large dipole moment and high polarizability, which result in strong dipole-dipole interactions between atoms. This makes a gas of Rydberg atoms an ideal system to study and simulate quantum may-body physics. By exciting ground-state atoms in an optical lattice to Rydberg states, we can realize a lattice of Rydberg atoms which is promising to reach a system of strong correlation, strong interaction, and low temperature.

In this poster, we present the current status of our experiment, the near-future goal of detecting and probing Rydberg atoms via electromagnetically induced transparency, and our work towards the realization of a lattice of Rydberg atoms.

P17 phase transition with gravitational-like interaction in a cloud of cold atoms

David Wilkowski

Thursday 05.00 PM, Foyer/Hallway, Panel 17 (EC number: 38)

We propose to use a cloud of laser cooled atoms in a 1D or 2D trap to investigate long range gravitational-like interaction. In 1D geometry, We give experimental evidences of such an interaction in a cold Strontium gas, studying the density profile of the cloud and its breathing oscillations [1]. In 2D, using theoretical arguments and numerical simulations, we show that, a transition to a collapsed state occurs below a critical temperature.

In addition and as a signature of the non equilibrium nature of the system, persistent particles currents, dramatically increasing close to the phase transition, are observed [2].

[1] M. Chalony, A. Olivetti, B. Marcos, J. Barré and D. Wilkowski, Phys. Rev. A **87**, 013401 (2013); [2] J. Barré, B. Marcos and D. Wilkowski, ArXiv 1312.2436.

P18 Bistability in bosonic terahertz lasers

Anastasiia Pervishko, Timothy C. H. Liew, Alexey Kavokin, Ivan Shelykh

Thursday 05.00 PM, Foyer/Hallway, Panel 18 (EC number: 39)

Efficient sources of terahertz radiation attract the attention of researchers from different scientific fields due to the various possibilities of application. However, the usage of modern THz sources is limited by the bulkiness and special working conditions. Quantum microcavities are offered to be used as an alternative source of THz radiation. Recently the possibility of realization of a THz emitter based on the radiative transition between 2p and 1s exciton states was predicted.

In this work we propose a theoretical model of a THz laser based on the 2p to 1s exciton transition in a semiconductor microcavity. We investigate the dynamics of the system at different values of the quality factor of the THz resonator. We analyse the effect of bistability in this system and observe a bistable behaviour of the THz photon concentration as a function of the external pump for the case of a medium-quality THz microcavity. This novel phenomenon is promising for many applications. One of them is a THz photon emission sensor based on this system.

P19 Experimental Estimation of the Dimension Witness of Quantum Systems

Hou Shun Poh, Tien Tjuen Ng, Yu Cai, Chen Ming Chia, Valerio Scarani, Christian Kurtsiefer

Thursday 05.00 PM, Foyer/Hallway, Panel 19 (EC number: 40)

The dimensionality of a system, the number of independent degrees of freedom needed to completely describe it, is one of the most basic concepts in science. Most of the theoretical models place assumptions on the dimensionality of a system. It would be desirable to assess the dimensionality of a system without assumptions. One such class of measurements are the dimension witnesses. They provide a lower bound on the dimensionality of a system by appealing to statistics from specific measurements. Here, we experimentally test a dimensional witness on a 4-dimensional photonic state in order to bound its dimensionality.

P20 Optical conductivity studies of Bi_2Te_3-Graphene composite in the terahertz range

Huanxin Xia, Meng Zhao, Chan La-O-Vorakiat, Elbert Chia

Thursday 05.00 PM, Foyer/Hallway, Panel 20 (EC number: 44)

The real part of the optical conductivity of the topological insulator Bi_2Te_3, single-layer-graphene (SLG), and Bi2Te3/SLG composite, all grown on p-doped Si substrate, were obtained using Terahertz time-domain spectroscopy (THz-TDS), in the temperature range 15 – 300 K and frequency range 0.3 - 3 THz. Both the Drude response, and three Raman-infrared active optical phonon modes, were observed: $E \approx 1\,\mathrm{THz}$, $A \approx 1.7\,\mathrm{THz}$ and $A \approx 2.7\,\mathrm{THz}$ [1,2]. The Drude contribution from SLG in the Bi2Te3/SLG composite was surprisingly suppressed above $\approx 80\,\mathrm{K}$, whose origin remains to be solved.

P21 Quantum Entanglement for Outer Space

Rakhitha Chandrasekara, Zhongkan Tang, Yue Chuan Tan, Sean Yau, Cliff Cheng, Christoph Wildfeuer, Alexander Ling

Thursday 05.00 PM, Foyer/Hallway, Panel 21 (EC number: 45)

We are working on polarization-entangled single photon pair sources which are to be hosted in satellite platforms, enabling quantum communication applications such as Quantum Key Distribution (QKD) at longer distances. It will open a pathway for a set of new type of quantum experiments which involve in microgravity environments. A widely accepted nano-satellite platform called the Cubesat is a cost-effective technology to bring a single photon source into the outer Space at the cost of limited resources such as volume, mass and power required for such a laboratory experiment. Our system is fully autonomous to conduct a single photon source verification experiment with on-board single photon detectors. Space environment puts many challenges on single photon sources and detectors such as temperature variations, radiation damage. Recently we checked the technology readiness of our Small Photon Entangling Quantum System (SPEQS) in a weather balloon which lofted the SPEQS to high altitude (around 35km). In our poster we will discuss how above mentioned challenges are addressed and the technology readiness of the SPEQS based on latest data available from the weather balloon test.

P22 Huge excitonic effects in a-MoO_3: from bulk to monolayer

Jiaxu Yan, Lei Liu, Jer-Lai Kuo, Zexiang Shen

Thursday 05.00 PM, Foyer/Hallway, Panel 22 (EC number: 47)

Although a-MoO_3 has been found widespread use in solid state microbatteries and heterogeneous catalysis, its electronic and particularly optical properties still have not been well established. The resulting computed in-plane polarized optical spectrum, obtained by solving the Bethe-Salpeter equation for many-body Green function, is in excellent agreement with experiment and has a strong anisotropy. A detailed analysis of the excitonic structures within the band gap shows strong excitonic effects with a significantly large binding energy assigned to the bound excitons. This provides an explanation for the observed‘optical gap’ contradictions between experiments and theories.

P23 Entanglement verification using witness bases

Jibo Dai, Yink Loong Len, Berge Englert, Leonid Krivitsky, Yong Siah Teo

Thursday 05.00 PM, Foyer/Hallway, Panel 23 (EC number: 59)

To determine whether a state is entangled or separable, one can achieve this by measuring witness operators which form an IC-POM [1]. We experimentally implement this idea for two-qubit photonic systems. By further introducing adaptive schemes, we demonstrate how to detect entanglement with the least tomographic effort. For states of different rank, strong agreement between experimental and theoretical results is observed.

[1] Phys. Rev. A 81, 052339 (2010)

P24 Particle shedding from coated magnetic microbubbles

Chon U Chan, Yu Gao, Chenjie Xu, Manish Arora, Claus-Dieter Ohl

Thursday 05.00 PM, Foyer/Hallway, Panel 24 (EC number: 60)

Nanoparticle-coated microbubbles have found applications for diagnostic imaging as well as drug delivery, yet the release of shell material due to ultrasonic excitation has not been studied in detail. We find that particles are ejected from the shell if the bubbles are driven resonantly with ultrasound. The bubble oscillation and the release of the particles are observed with high-speed photography while floating in microfluidic channels. The nanoparticles are shed when the bubble wall acceleration exceeds a threshold. When bubbles are excited into shape oscillations the particle shedding is observed at the velocity antinodes of the bubble surface. Particle release and transport is modelled with a force balance, considering inertia of the particle, the oscillatory fluid flow created by bubble oscillation, and the viscous force acting on the particle. We also demonstrate the ability to control the location of microbubbles in liquid using a diverging magnetic field and an optical feed-back loop. Then the magnetic microbubbles can be stabilized and translated in a three dimensional bubble trap.

P25 Towards solid-state magnetometry with nitrogen-vacancy centre

Yue Sum Chin, Alessandro Cerè, Christian Kurtsiefer

Thursday 05.00 PM, Foyer/Hallway, Panel 25 (EC number: 61)

We report on the observation of photoluminescence from a single nitrogen-vacancy (NV) centre in diamond at room temperature. A diamond sample is optically excited by a laser of wavelength 532 nm and the resulting fluorescence is collected. In order to selectively address a single NV centre, we set up a scanning confocal microscope with resolution approaching the diffraction limit. We distinguish NV centres from other colour centres in diamond by observing spectrum of the fluorescence. The signature zero phonon line (ZPL) at 637 nm and the broadened vibrational spectrum identifies the emitter as a

NV centre. We confirm the observation of a single NV centre by performing a Hanbury-Brown-Twiss measurement on the fluorescence. The measurement shows a second order correlation function $g^{(2)}(0) = 0.16$. This indicates that only a single NV centre is being observed. Finally, we present our progress towards using single NV centre as microscopic magnetic probe by using magnetic properties of its electronic ground states.

P26 A high flux source for ultracold Strontium atoms

Tao Yang, Chang Chi Kwong, Pramod Mysore Srinivas, Chia Zhong Yi, Frederic Leroux, Kanhaiya Pandey, David Wilkowski

Thursday 05.00 PM, Foyer/Hallway, Panel 26 (EC number: 62)

Sr has two optical transitions from the ground state. One at 461 nm (blue) is strong whereas the other at 689 nm (red) is 4000 times weaker. This weak transition allow us to study the transient and coherent effects in the transmission through cold Sr atoms, as well the artificial gauge fields.

In this poster, we present our experimental set-up to produce high flux of cold Sr atoms for the above goals . We first mechanically and optically collimate the Sr atoms and then slow them using Zeeman slower. Then we guide these slowed atoms into the ultra-high vacuum (10^{-12} mbar) using the blue 2D MOT. Further using blue transition we cool and trap the atoms simultaneously in the 3D MOT as well as in the magnetic trap. The temperature at this stage happens to be of order few mK. Using the weak transition we further cool the atoms upto few microK.

P27 Terahertz Conductivity Study of a Lead Halide Perovskite: $CH_3NH_3PbI_3$

Chan La-O-Vorakiat, Jeannette M. Kadro, Maria-Elisabeth Michel-Beyerle, Elbert Chia

Thursday 05.00 PM, Foyer/Hallway, Panel 27 (EC number: 63)

We study the optical conductivity in the terahertz range of $CH_3NH_3PbI_3$ – a promising hybrid organic-inorganic perovskite material for the next generation of solar cell devices [1,2]. The conductivity spectra contain peaks due to phonon-mode resonances around 0.9 and 1.9 THz. We use two-Lorentz model [3] to analyze the data across a broad sample temperature range (10-400 K) and extract material parameters such as mobility and oscillator resonance frequencies. We observed the discontinuities in the fitting parameters due to structural phase transition from β to γ phase at 165 K.

References: [1] M. M. Lee, et al. Science, 338, 643 (2012); [2] H. S. Kim, et al. Scientific Reports, 2, 591 (2012); [3] X. Zou, et al. AIP Advances, 2, 012120 (2012).

P28 Laser system for the production of ^{6}Li-^{40}K dipolar ground state molecules

Johannes Gambari, Sambit Pal, Mark Lam, Markus Debatin, Kai Dieckmann

Thursday 05.00 PM, Foyer/Hallway, Panel 28 (EC number: 64)

Heteronuclear ground-state molecules with relatively low dipole moment have been successfully created through coherent transfer from highly excited states [1,2]. We present a laser system for the ground state transfer of the previously presented Bosonic ^{6}Li-^{40}K, Feshbach molecules [3]. We achieve an absolute stability of 5 kHz between both sub-kHz lasers.

The wavelengths required for the Raman laser system are 767 nm and 522 nm [4,5], which are roughly 250 nm apart and generated by two distinct external cavity diode lasers (ECDLs). For an efficient ground state transfer, we require sub kHz linewidths and an absolute stability of a few kHz. These requirements have been previously achieved [1] by locking two lasers to a frequency comb. In our case achieving a heterodine optical beat in the blue-green region of the spectrum is challenging because of the lower spectral response of the photodiodes in this region as well as the lower and unstable power of the needles in this region of the comb. A common alternative solution is locking two lasers to a piezo-tunable transfer cavity. Lasers have been locked to such a cavities with frequency noise below $30\,\mathrm{Hz}/\sqrt{\mathrm{Hz}}$ for Fourier frequencies above 4 mHz[6]. When locking such cavities to atomic transitions (via saturated absorption spectroscopy), one typically obtains linewidths of 10 s of kHz[6], which does not meet our requirements.

In this work we demonstrate a comb-enabled transfer lock scheme that does not require a heterodine beat with the comb in the blue-green region. We lock two ECDLs to the same Fabry Perot resonator (FPR). We use an EOM between each ECDL and the laser cavity to perform the Pound Drever Hall lock; and at the same time by driving the EOM with a Nonlinear Transmission line we are able to also shift the frequency of the locked ECDL[7]. Via an optical lock, we lock a commercial frequency comb (FC1500) to the 767 nm ECDL and use a frequency counter referenced to a high performance GPS referenced frequency standard to detect the drift in repetition rate of the FC1500. This drift, scaled by the needle order of the comb directly gives the frequency correction that needs to be applied to both lasers, which is done via the EOM.

References: [1] A. K. Ni, Science 322, 231 (2008); [2] M. Debatin PhD thesis (2013); [3] A-C Voigt et al., Phys. Rev. Lett. 102, 020405 (2009); [4] E. Tiemann et al., PRA 79, 042716 (2009); [5] R-A. Allouche, private communication; [6] K. Möhle, PhD thesis (2013); [7] R. Kohlhaas et al. Opt. Lett. 37, No. 6 (2012)

P29 Direct and indirect protocols for distribution of entanglement

Alessandro Fedrizzi, Margherita Zuppardo, Mauro Paternostro, Tomasz Paterek

Thursday 05.00 PM, Foyer/Hallway, Panel 29 (EC number: 65)

Most applications of quantum entanglement, particularly in the field of quantum communication, rely on the possibility to generate entangled states between two parties that are far away from each other. However, this is usually not a trivial task, especially in the presence of noisy channels, which is almost unavoidable in practical cases. For this reason, it is a very interesting challenge to find new protocols that allow distributing entanglement between two distant laboratories. Some of these protocols are rather counterintuitive: for instance, it has been shown [1] that it is possible to generate entan-

glement between distant parties without having to carry any. The existence of protocols involving entanglement distribution via separable (unentangled) states (EDSS) highlights a surprising and unique characteristic of quantum entanglement, understanding which improves our knowledge about quantum mechanics. However, questions concerning the practical possibility and real helpfulness of such protocols were not addressed until very recently. I will describe one of the first experiments realizing an EDSS protocol [2]. In such experiment, we entangled two distant laboratories by using three initially separable photonic qubits, A, B and C, prepared in a particular mixed state. The entanglement is distributed by using C as a carrier that, although interacting with A through a quantum gate, remains separable with both A and B at all stages. We are able, in this way, to generate a measurable amount of distillable entanglement between the laboratory holding A and the one containing B and C. I will also address the problem on the convenience of EDSS protocols over other ways of generating entanglement. For example, an alternative, natural way would be entangling two particles in the same place, and then sending one to the other lab (direct distribution). It is an easy conjecture that, if the two systems are initially maximally entangled, this will generate the largest possible amount of entanglement that the noisy channel allows. However, generating maximally entangled states can be a rather expensive task. We show that EDSS protocols can increase the amount of entanglement shared between the parties after a direct distribution, in some cases when maximally entangled states are not available. These results open up new horizons for the practical realization of quantum communication and other scenarios that involve quantum entanglement.

[1] T. S. Cubitt, F. Verstraete, W. Dür, and J. I. Cirac, Phys. Rev. Lett. 91, 037902 (2003); [2] A. Fedrizzi, M. Zuppardo, G. G. Gillett, M. A. Broome, M. P. Almeida, M. Paternostro, A. G. White, and T. Paterek, Phys. Rev. Lett. 111, 230504 (2013)

P30 Realtime Visualization of Surface Nanobubbles Dynamics

Manish Arora, Chon U Chan, Beng Hau Tan, Claus-Dieter Ohl

Thursday 05.00 PM, Foyer/Hallway, Panel 30 (EC number: 68)

Nanobubbles nucleate and reach a stable state on the solid-liquid interface after ethanol-water exchange. Understanding the thermodynamic stability beyond their formation requires observation of their dynamical response. Total internal reflection microscopy [1] allows resolving the dynamics of nanobubbles, i.e. their formation, shrinkage, and coalescence. Here we report on nanobubble dynamics induced by the exchange process in a microfluidic channel on a glass surface. Formation of attached nanobubbles at 50 frames per second is observed during the transition from water-to-ethanol as well as ethanol-to-water. Bubbles dissolve within a second in ethanol but persist in water. Though new nanobubbles keep appearing over several seconds, no further change in their size is observed. However, we find occasionally spontaneous merging of neighbouring nanobubbles which we relate to the liquid flow. Study is complimented with Atomic Force Microscopy observation of nanobubbles after the water-ethanol-water exchange at a higher spatial resolution but much lower temporal resolution. Though the role of tip

interaction cannot be ruled out; dynamic events of nanobubble emergence, merger, and disappearance are observed in initial 15 minutes of after exchange process.

[1] Chan and Ohl, Phys. Rev Lett. 109, 174501 (2012)

P31 Single mode emission and improved sensor sensitivity via coupled fiber lasers

Van Duong Ta, Rui Chen, Handong Sun

Thursday 05.00 PM, Foyer/Hallway, Panel 31 (EC number: 70)

Whispering gallery mode (WGM) optical cavities are interesting structures due to their high quality (Q) factor and small mode volume. They offer strong optical confinement for fundamental study of light-matter interaction, quantum electrodynamics and applications such as optical switches, filters and lasers. For a laser source, single mode emission is the most important case because it is required for optical information processing and integrated chips. However, single mode operation based on single WGM cavity can be obtained only by reducing cavity size. This technique leads to fabrication difficulty and deteriorates the laser Q factor. Herein, we demonstrate high Q single mode lasing by coupling two asymmetric fibers. Thanks to the Vernier effect, the single mode is generated by suppression of lasing modes, and therefore, without affecting the laser Q factor. In our work, the spectral linewidth is about 0.09 nm, corresponding to laser Q around 7×10^3, which is several times higher compared with previous reports on polymer fiber lasers. More interestingly, the coupled structure exhibit improved sensitivity compared with the isolated one when employed them for refractive index sensing. Our finding explores the favorable of coupled fiber cavities for applications in flexible photonic devices and sensors.

P32 Geometrical adiabatic qubit and artificial magnetism in a four-level tripod system.

Frederic Leroux

Thursday 05.00 PM, Foyer/Hallway, Panel 32 (EC number: 72)

A four-level tripod system driven continuously by three lasers has a pair of dark states with zero energy which can be used to encode a single qubit. We show that by tuning the phases of two lasers adiabatically, the state vector of the atom stays within the dark states eigenspace. In this way, we can define a U(2) geometrical gate for this qubit. An optically synthesized non-Abelian Gauge potential connected to this geometrical gate emerges.

We will use magnetic sublevels of one of the hyperfine state of Strontium 87 for this tripod configuration. We expect the dynamics of these neutral atoms in this artificial Gauge field to mimic the action of a kind of Lorentz force.

P33 The impact of annealing on low temperature thermally reduced graphene oxide

Garen Kwan

Thursday 05.00 PM, Foyer/Hallway, Panel 33 (EC number: 73)

Current techniques of producing reduced graphene oxide (rGO) from graphene oxide (GO) involve either high temperatures ($> 1173\,\mathrm{K}$) or the use of harmful chemicals such as hydrazine. While attempts at low temperature reduction have required the use of secondary chemicals that then introduce new levels of complexity to the material system. It is shown that, compared to unannealed films, performing an annealing step on GO prior to low temperature thermal reduction (at $573\,\mathrm{K}$) halves the sheet resistance of the resulting film while retaining a similar optical transmittance value. To understand this, ab-initio calculations were performed using the Vienna Ab-initio Simulation Package. The calculations revealed that the annealing step allows oxygen groups to migrate across the surface of the GO flake into a configuration of lower energy. This configuration, consisting of oxygen-rich domains surrounded by tracts of oxygen-free graphene, reduces the formation of defects in the rGO film during the thermal reduction step, hence explaining the better electrical conductivity observed. Characterization measurements performed on annealed GO solutions show an increase in the UV-Vis absorption spectra at $1.16\,\mathrm{eV}$ as well as a red shift of the position of the absorption peak (from $2.93\,\mathrm{eV}$ to $2.04\,\mathrm{eV}$) that occurs linearly with respect to annealing time over the course of 50 hours. This supports the hypothesis that a preferred arrangement of the oxygen groups on the GO is obtained during annealing. This finding will aid in developing new low temperature techniques of producing rGO films and solutions for uses in applications such as battery technology and transparent electrodes.

P34 Dynamics of localized waves in 1D random potentials: statistical theory of the coherent forward scattering peak

Kean Loon Lee, Benoit Gremaud, Christian Miniatura

Thursday 05.00 PM, Foyer/Hallway, Panel 34 (EC number: 74)

As recently discovered [PRL **109** 190601(2012)], Anderson localization in a bulk disordered system triggers the emergence of a coherent forward scattering (CFS) peak in momentum space, which twins the well-known coherent backscattering peak (CBS) observed in weak localization experiments. Going beyond the perturbative regime, we address here the long-time dynamics of the CFS peak in a 1D random system and we relate this novel interference effect to the statistical properties of the eigenfunctions and eigenspectrum of the corresponding random Hamiltonian. Our numerical results show that the dynamics of the CFS peak is governed by the logarithmic level repulsion between localized states, with a time scale that is approximately twice the Heisenberg time. This is in good agreement with recent findings based on the nonlinear σ-model. In the stationary regime, the width of the CFS peak in momentum space is inversely proportional to the localization length, reflecting the exponential decay of the eigenfunctions

in real space, while its height is exactly twice the background, reflecting the Poisson statistical properties of the eigenfunctions. Our results should be easily extended to higher dimensional systems and other symmetry classes.

P35 (poster withdrawn)

Paola Lova, Valentina Robbiano, Franco Cacialli, Davide Comoretto, Cesare Soci

Thursday 05.00 PM, Foyer/Hallway, Panel 35 (EC number: 77)

(none)

P36 CuO/ZnO Heterojunctions

Daniele Cortecchia, Diana Gisell Figueroa Del Valle, Ilka Kriegel, Tingchao He, Jun Yin, Majid Panahandeh-Fard, Manoj Kumar, Handong Sun, Francesco Scotognella, Cesare Soci

Thursday 05.00 PM, Foyer/Hallway, Panel 36 (EC number: 79)

Copper oxide semiconductors are widely studied as light absorbers in solar cells and photoelectrochemical cells (PEC) since they are abundant, inexpensive, solution-processable and environment-friendly. Among the copper oxides, cupric oxide (CuO) is highly stable and highly absorbing throughout the solar spectrum. Being intrinsically p-type due to the presence of copper vacancies, with a direct band gap of 1.0-1.5 eV and an indirect band gap of 2.0-3.3 eV, it may be easily coupled to n-type materials like ZnO to produce low-cost solar cells. Nevertheless, CuO has rarely been considered for photovoltaic applications and the few CuO/ZnO heterojunction devices reported in the literature suffered from extremely low efficiency. Here we fabricate ZnO/CuO heterojunctions by a simple and scalable method that combines sol-gel spin coating and spray pyrolysis. We determine morphology and composition of the oxide films by SEM, AFM and XRD and study their optical and transport properties by UV-Vis, photoluminescence, and photocurrent spectroscopy. Charge transfer across the CuO/ZnO heterojunction is also probed by femtosecond transient absorption. We find that, while ZnO acts as an efficient charge extraction layer, the formation of long lived trapped states limits electron transport in the CuO thin film. Therefore, even if ZnO promotes depopulation of electrons in the trapped states, trap states seem to be the main factor limiting electron transport in the heterojunction.

P37 III-V Core-Shell Nanowire Photodetector

Xing Dai, Sen Zhang, Zilong Wang, Giorgio Adamo, Hai Liu, Yizhong Huang, Christophe Couteau, Cesare Soci

Thursday 05.00 PM, Foyer/Hallway, Panel 37 (EC number: 80)

III-V semiconductor nanowires have gained intense attention for optoelectronic and photovoltaic applications thanks to their direct bandgap, versatility in bandgap engi-

neering and high charge carrier mobility. To achieve high responsivity, large photoconductive gain, fast response time, and low noise in nanowire photodetectors, structures of coaxial p-type/n-type (p/n) or p/intrinsic/n (p/i/n) coaxial junctions, phototransistors, and back-to-back Schottky barrier devices were proposed and investigated. Here we present the design and implementation of a core-shell GaAs/AlGaAs type I nanowire heterostructure where a high-density, cylindrical two-dimensional electron gas is formed along the nanowire axis to promote photoinduced charge dissociation and prolong carrier lifetime. A single nanowire photodetector realized by forming selective contacts to the shell and the core regions reveals strong photoresponsivity in the visible to near infrared spectral region at room temperature, consistent with electromagnetic and transport simulations of optical absorption and photoconductive characteristics of the device.

P38 Charge Modulation Spectroscopy of p-type and n-type Conjugated Polymers

Xin Yu Chin, Jun Yin, Zilong Wang, Alessandro Luzio, Daniele Fazzi, Mario Caironi, Cesare Soci

Thursday 05.00 PM, Foyer/Hallway, Panel 38 (EC number: 82)

Infrared Charge Modulation Spectroscopy (IR-CMS) is an electro-optical technique that utilizes interfacial doping to access polaranic and vibrational absorption features of conjugated polymers. We use IR-CMS to study charge carrier distribution and transport in the nanometer-thick accumulation layer of polymer FETs. By taking advantage of the high specificity and strong oscillator strength of Infra-Red Active Vibrational (IRAV) modes and low-energy polaron bands probed in this spectral region, IR-CMS measurements implemented with a confocal microscope allow quantitative estimate of charge carrier densities and mapping of spatial carrier distribution in different working regimes of FET devices. Both p-type poly(3-hexylthiophene) (P3HT) and n-type N2200 (Polyera Ink) transistors were optimized to study CMS spectroscopic signature of positive and negative polaron. Thanks to the underlying equivalence of interfacial and photoinduced doping, CMS charge-induced absorption signals showed one-to-one correspondence to photo-induced absorption. Density Functional Theory (DFT) calculations, Raman and linear vibrational spectroscopy were also carried out to assign the spectral features of IR photoinduced absorption and CMS measurements of both prototype polymers. We demonstrate that IR-CMS mapping is a unique tool to study polaron accumulation, trapping, and transport in polymer FETs.

P39 Towards quantum nanodevices: example of plasmonic rings

Nancy Rahbany, Wei Geng, Rafael Salas-Montiel, Sylvain Blaize, Renaud Bachelot, Christophe Couteau

Thursday 05.00 PM, Foyer/Hallway, Panel 39 (EC number: 88)

There is a growing interest nowadays in the study of strong light-matter interaction at the nanoscale. Using plasmonics, nanooptics and metamaterials, there is an important

drive towards enhancing such an interaction. In this work, we aim to excite surface plasmon polaritons (SPPs) using circular ring gratings where light-matter interaction can be studied at the nanometer scale. This can be implemented to study the fluorescence enhancement of single emitters placed inside the rings. So upon integrating single-photon sources with plasmonic structures, the emitter's enhanced Purcell factor in the weak coupling regime can be obtained. Ring gratings with different designs and diameters were fabricated on Si and glass substrates using Electron Beam Lithography (EBL). The structures were studied using a fiber coupling setup where an incident fiber is used to illuminate the ring grating at a certain position. As a result, excited SPPs propagate along the ring diameter and couple again at an opposite position on the grating. FDTD simulations were done using Lumerical software in order to calculate the optimized angle of incidence. We will present far-field as well as near-field optical characterisations of these structures. The next step in this work will be to place single emitters inside the plasmonic rings to observe their spontaneous emission enhancement.

P40 Dynamics of Phase transformation in chemically exfoliated tungsten sulfide

Kiran Kumar Amara, Rajeev Kumar

Thursday 05.00 PM, Foyer/Hallway, Panel 40 (EC number: 90)

Exfoliation by Lithium ion intercalation induces polymorphism in Molybdenum disulfide. The transition from metastable 1T phase (octahedral) to thermodynamically stable 2H (trigonal prismatic) in the chemically exfoliated samples was reported in MoS_2 with annealing ($> 300\,^{\circ}C$) [1]. The existence of coherent atomic and electronic heterostructures (2H and 1T) in single layer of MoS_2 was also reported [2]. Here we achieved production of single layers of WS_2 using $LiBH_4$ according to the method reported by Tsai et al and studied the polymorphs under STEM [3]. We observed simultaneous existence of different phases (2H, 1T, 1T') by STEM in chemically exfoliated WS_2. We also observed the phase transformation form 1T' to 1T under electron beam irradiation.

References: [1] Eda, G.; Yamaguchi, H.; Voiry, D.; Fujita, T.; Chen, M.; Chhowalla, M., Photoluminescence from chemically exfoliated MoS_2. Nano Lett 2011, 11 (12), 5111-6; [2] Eda, G.; Fujita, T.; Yamaguchi, H.; Voiry, D.; Chen, M.; Chhowalla, M., Coherent Atomic and Electronic Heterostructures of Single-Layer MoS_2. ACS Nano 2012, 6 (8), 7311-7317; [3] Tsai, H.-L.; Heising, J.; Schindler, J. L.; Kannewurf, C. R.; Kanatzidis, M. G., Exfoliated−Restacked Phase of WS2. Chemistry of Materials 1997, 9 (4), 879-882.

P41 Monte Carlo algorithm for optimal error regions

Jiangwei Shang, Hui Khoon Ng, Yi-Lin Seah, Xikun Li, David Nott, Berthold-Georg Englert

Thursday 05.00 PM, Foyer/Hallway, Panel 41 (EC number: 93)

In our previous work, we have found a simple construction of optimal error regions for quantum state estimation. The optimal choices for two types of error regions—the

maximum-likelihood region, and the smallest credible region—are both concisely described as the set of all states for which the likelihood (for the given tomographic data) exceeds a threshold value, i.e., a bounded-likelihood region (BLR). Now the problem remains to evaluate the multi-dimensional integrals for the size and credibility of BLRs. For this, we need good sampling strategies. Markov-chain Monte Carlo (MCMC) methods, such as the Metropolis-Hastings algorithm, suggest themselves. So in this work, we focus on exploring various efficient MC algorithms as well as their potential applications.

P42 Measurement-Based Quantum Computation with Two-Body Qubits via Adiabatic Evolution

Thi Ha Kyaw, Ying Li, Leong Chuan Kwek

Thursday 05.00 PM, Foyer/Hallway, Panel 42 (EC number: 94)

A cluster state cannot be a unique ground state of a two-body interacting Hamiltonian. Here, we propose the creation of a cluster state of logical qubits encoded in spin-1/2 particles by adiabatically weakening two-body interactions. The proposal is valid for any spatial dimensional cluster states. Errors induced by thermal fluctuations and adiabatic evolution within finite time can be eliminated ensuring fault-tolerant quantum computing schemes.

P43 Oxide Nanostructures Hyperbranched with Thin and Hollow Metal Shells for High-Performance Nanostructured Battery Electrodes

Xinhui Xia, Hongjin Fan

Thursday 05.00 PM, Foyer/Hallway, Panel 43 (EC number: 98)

High-performance electrochemical energy storage (EES) devices require the ability to modify and assemble electrode materials with superior reactivity and structural stability. Herein, we report the fabrication of different oxide/metal core-branch nanoarrays with adjustable components and morphologies (e.g., nanowire and nanoflake) on different conductive substrates. The hollow metal branches (or shells) wrapping around oxide cores are realized by electrodepositon using ZnO nanorods as sacrificial template. In battery electrode application, the thin hollow metal branches can provide a mechanical protection of the oxide core and a highly conductive path for charges. As a demonstration, arrays of Co_3O_4/Ni core-branch nanowires are evaluated as anode for lithium ion batteries. It is shown that the thin metal branches evidently improve the electrochemical performance with higher specific capacity, rate capability and capacity retention.

P44 A portable, all-optical magnetometer with high sensitivity

Herbert Crepaz, Li Yuan Ley, Rainer Dumke

Thursday 05.00 PM, Foyer/Hallway, Panel 44 (EC number: 104)

We present a portable, atomic magnetometer based on nonlinear magneto-optical rotation with frequency and amplitude-modulated light. This method enables sensitive field measurements of various test samples without the need of calibration or cryogenic temperatures. We demonstrate a sensitivity of $10^{-14}\,\mathrm{T}/\sqrt{\mathrm{Hz}}$ and show preliminary measurements to discern possible magnetoactivity of the arthropod Periplaneta Americana (American cockroach). This would have important implications for the theory of magnetoreception in invertebrates.

P45 Ramsey-Interferometer Gravimeter

Fong En Oon, Mirco Sierce, Rainer Dumke

Thursday 05.00 PM, Foyer/Hallway, Panel 45 (EC number: 106)

In this project we are constructing a Ramsey-interferometer type of gravimeter to measure the local g. It can be used in various practical applications like geophysics, volcanology, mineral prospecting, etc. The system has currently reached an accuracy of $10^{-6}\,\mathrm{g}$ and is now working in achieving the designed accuracy of $10^{-8}\,\mathrm{g}$.

P46 Entanglement of a 2-qubit system coupled to a bath of quantum spin glass

Chee Yeong Koh, Leong Chuan Kwek

Thursday 05.00 PM, Foyer/Hallway, Panel 46 (EC number: 108)

We study the quantum entanglement (concurrence) of a 2-qubit system coupled to a small spin glass bath of 2 to n $\geq$ 4 qubits. The bath is described by the quantum XX Heisenberg model with random J coupling and varying magnetic field h. We look at the dynamics of the steady state average concurrence for the system and obtain a general formula to describe the concurrence with J = 0 and h = 0 for n bath sites. The physics of 2-qubit system coupled with n bath sites for J = 0 is analytically described for small n. The result for large n was numerically found to be qualitatively similar. For small fluctuation in J, a mean steady state average concurrence of about 0.5 is obtained.

P47 GaAs/AlGaAs nanowires for optoelectronics

Aurélien Olivier, Christophe Wilhelm, Christophe Couteau, Cesare Soci

Thursday 05.00 PM, Foyer/Hallway, Panel 47 (EC number: 109)

Growth mechanisms and their influence on morphology of semiconductor nanowires have been largely studied. Thanks to their 1D geometry, nanowires exhibit unique properties that can overcome technological and physical issues encountered in electronic, optoelectronic and photonic applications [1]. For example, III-V nanowires are widely considered for high-speed field-effect transistors and high photoresponsivity photodetectors [2]. Surface passivation of GaAs, for instance with AlGaAs, is crucial to reduce surface states and prevent oxidation, which are known to degrade GaAs properties,

e.g. reducing electron mobility and increasing Auger recombination [3]. In this work we present the growth and characterization of GaAs/AlGaAs/GaAs core/double shell nanowires grown by Metal Organic Chemical Vapor Deposition (MOCVD). The GaAs core is grown by the vapour-liquid-solid (VLS) mechanism at 400°C and the double shell at higher temperature (700°C) by conformal epitaxy. Photoluminescence of nanowires transferred onto a Si host substrate demonstrates the effectiveness of the double shell layers for surface passivation and indicates the potential of such heterostructures for photodetection and light emission applications [4].

[1] P. Yang et al., Semiconductor nanowire: what's next? Nano Letters, 10, 1529-1536 (2010); [2] C-C. Chang, et al., Electrical and optical characterization of surface passivation in GaAs nanowires, Nano Letters, 12, 4484-4489 (2012); [3] X. Dai et al., GaAs/AlGaAs nanowire photodetector, to be submitted; [4] A. Larrue et al., Monolithic integration of III-V nanowire with photonic crystal microcavity for vertical light emission. Optics Express, 20, 7758-7770 (2012).

P48 Manipulating the terahertz polarization states

Longqing Cong, Ranjan Singh, Jiaguang Han, Jianqiang Gu, Zhen Tian, Weili Zhang

Thursday 05.00 PM, Foyer/Hallway, Panel 48 (EC number: 111)

As investigations into potential applications of terahertz science and technology boom, there is an increasing demand for improved terahertz optical components such as the polarization control devices. Here we discuss different metamaterial device designs that have shown properties of perfect linear polarization rotation and linear to circular polarization conversion at narrowband as well as broadband terahertz frequencies.

P49 Towards simulating physics with Ion Traps

Debashis De Munshi, Riadh Rebhi, Manas Mukherjee

Thursday 05.00 PM, Foyer/Hallway, Panel 49 (EC number: 112)

We propose to use ion traps for experimenting with simulating various physical problems. We propose a novel ion trap design that allows us to perform non-abelian to abelian transition on trapped ions. We also propose the said trap to perform simulation of Bose-Hubbard model using the phonon modes of a linear chain of ions.

P50 Explicating the Effects of Single Silver Nanowire on the Performance Improvement in Plasmonic Organic Solar Cells

Xinfeng Liu, Bo Wu, Qing Zhang, Jing Ngei Yip, Guannan Yu, Qihua Xiong, Nripan Mathews, Tze Chien Sum

Thursday 05.00 PM, Foyer/Hallway, Panel 50 (EC number: 115)

The origins of the performance improvement in hybrid plasmonic organic solar cells are often mired in a complex interplay of various effects (e.g. light scattering, localized

surface plasmon resonances, exciton-plasmon energy transfer etc.). To disentangle the contributions from these effects, herein we investigate the single silver nanowire effects on the performance improvement of polymer bulk heterojunction solar cells using spatially-resolved transient absorption and time-resolved photoluminescence spectroscopy as well as electrical measurements. A maximum enhancement of the solar cell efficiency $\approx 38\%$ is obtained when the incident polarization is perpendicular to the long axis of silver nanowire, as a result of transverse surface plasmon enhanced exciton and polaron densities. The efficiency improvement is predominantly attributed to higher absorbance and scattering induced by the localized surface plasmon rather than direct surface plasmon-exciton energy transfer or coupling. Finite-difference time-domain simulation is further conducted to validate these findings. Our results are beneficial to the design of highly efficient hybrid plasmonic polymer solar cell devices.

P51 Ni_3S_2@MoS_2 Core/Shell Nanowire Arrays on Ni Foam for High-performance Electrochemical Energy Storage

Jin Wang, Zexiang Shen, Jianyi Lin

Thursday 05.00 PM, Foyer/Hallway, Panel 51 (EC number: 120)

A green, scalable and one-step solution strategy is developed to construct one-dimensional (1D) hierarchical core/shell structures on Ni foam, which is composed of MoS_2 nanosheets grown on Ni_3S_2 nanowires (denoted as Ni_3S_2@MoS_2). When they are tested as supercapacitor electrodes, the Ni_3S_2@MoS_2 heterostructure exhibits 2 to 4 times the capacitance compared to bare Ni_3S_2 sample. The enhancement is ascribed to the robust hierarchical core/shell structures which provides an increased reaction area and a close contact of electrolyte with the active material. In addition, a highly conductive 1D core material endows the quick transport of electrons along Ni_3S_2 nanowires to Ni foam. It is prospected that such novel hybirds can offer great potential promise in large-scale energy storage device applications.

P52 Raman Spectroscopy Study of Lattice Vibration and Crystallographic Orientation of Monolayer MoS_2 under Uniaxial Strain

Wang Yanlong, Cong Chunxiao, Qiu Caiyu, Yu Ting

Thursday 05.00 PM, Foyer/Hallway, Panel 52 (EC number: 127)

Molybdenum disulfide (MoS_2), a typical candidate of transition metal dichalcogenides (TMDs) with layered structure has been shown to possess unique optical, electrical and mechanical properties. Here we report a systematic micro-Raman spectroscopy study of monolayer MoS_2 under controllable uniaxial tensile strain. Our experimental observation reveals that the E_2g^1 optical phonon mode is sensitive to the in-plane uniaxial strain while the A1g mode is inert to the strain. When the strain is sufficient high (i.e. $> 1\%$ in this work) to break the lattice symmetry, such doubly degenerate E_2g^1 mode splits into two subbands, named $E_2g^{(1+)}$ and $E_2g^{(1-)}$, according to their vibration energies. Our polarization dependent Raman spectroscopy investigation further indicates that the

polarizations of the scattered light from these two subbands are linear and orthogonal. Furthermore, the polar angles for the maxima and minima of the intensities of these two subbands are strongly determined by the crystallographic orientation relevant to the strain direction as predicted by the theoretical analysis. The Grüneisen parameter for E_2g^1 phonon of monolayer MoS_2 is also studied. Our findings firmly demonstrate that Raman spectroscopy is a powerful probe to monitor the amount of strain, identify the crystallographic orientation, and investigate mechanical properties of 2D transition metal dichalcogenides, such as MoS_2.

P53 Transport properties of monolayer MoS2 grown by chemical vapour deposition

Shunfeng Wang, Hennrik Schmidt, Goki Eda

Thursday 05.00 PM, Foyer/Hallway, Panel 53 (EC number: 133)

Atomically thin crystals of transition metal dichalcogenides (TMD) exhibit a board range of optical and electronical properties which make them interesting for basic research as well as applications. The success in the growth of monolayer MoS2 via chemical vapor deposition (CVD) has opened up prospects for large scale implementation into thin film electronic and optoelectronic devices. We investigate the electronic transport properties of individual crystallites of high quality CVD-grown monolayer MoS2. After careful annealing steps, we observe a clear signature of metallic conduction at high doping densities, previously only reached by topgating. The different scattering mechanisms are analysed and it is shown that the short-range scattering plays a dominant role in the highly conducting regime at low temperatures where mobility saturates.

6 Technical Sessions

6.1 T1 Two-dimensional Materials

This session will be held on Wednesday, February 26, from 01.30 PM to 03.10 PM. Venue for this session is Rooms 1+2. Time allocated for invited talks is 25 min speaking time, plus 5 min Q&A, and time allocated for contributed talks is 15 min speaking time plus 5 minutes Q&A.

T1.1 Light-matter interaction in 2D materials: from graphene to TMDs (INVITED)

Ting Yu

Wednesday, February 26, 01.30 PM, Rooms 1+2

Graphene and other atomically thin transition metal dichalcogenides (TMDs), as exceptional two dimensional materials, possess extremely promising potential for fundamental studies and practical applications. Here we report our studies on 2D materials such as graphene, MoS_2, $TaSe_2$ and WS_2. Photons, electrons, phonons and the interaction among them are systematically investigated through various optical probes. The results presented here are highly relevant to the application of 2D materials in nanoelectronic devices and help in developing a better understanding of the physical and electronic properties of those 2D materials.

T1.2 Atomically thin $MoSe_2$ film: Synthesis, optical and electrical properties, and electronic device applications (INVITED)

M. Iqbal Bakti Utama, Xin Lu, Qihua Xiong

Wednesday, February 26, 02.00 PM, Rooms 1+2

We have synthesized atomically thin film of $MoSe_2$ with chemical vapor deposition (CVD) method in large area, reaching 1x1 cm2, at monolayer and few-layer level. We observed that the CVD-$MoSe_2$ exhibited excellent optical properties. From Raman spectroscopy, both monolayer and bilayer exhibit strong and layer-sensitive peaks. Breathing mode and shear mode show observable shifts with increasing thickness. Furthermore, the low-frequency interlayer shear mode was identified in bilayer, while it disappears in monolayer because of the nature of interlayer vibration. On photoluminescence (PL) spectroscopy, we have detected strong emission from A exciton at room temperature. The dark emission from B exciton can also be observed with a splitting energy of 200 meV from A exciton. Temperature-dependent PL and optical absorption measurements further confirm the high quality of CVD-$MoSe_2$. At low temperature, negatively charged A- exciton emission appears with a binding energy of $\approx 20\,\text{meV}$. To complement the synthesis efforts, we have also developed a patterning method with SU-8 resist that circumvents the inertness of layered transition metal dichalcogenides in wet etchant and the complexity of available dry etching methods. E-beam lithography (EBL) exposure on SU-8 improves the adhesion of the resist onto the underlying 2D material, such that the 2D materials will also be removed when the developed SU-8 resist is dissolved. With this patterning method, we have been able to pattern CVD-grown films of $MoSe_2$ into

ribbon-shaped conduction channel for back-gated field effect transistors that avoids the current leakage due to defects on the gate oxide. Detailed temperature-dependence electrical characterizations shows that the carrier transport on $MoSe_2$ follows Mott variable range hopping, suggesting carrier localization due to disorder produced within the sample. Nevertheless, the electrical properties of the CVD-grown $MoSe_2$ sample are still comparable to among the performance of CVD-grown MoS_2: the field effect transistor (FET) action from $MoSe_2$ exhibited ambipolar behavior with electronic mobility of $0.02\,cm^2/V.s$ and 102 on-off ratio with just 37.5 V gate overdrive at room temperature. In addition, a top-gated inverter with gain larger than unity was fabricated succesfuly by implementing the patterning method on CVD-grown $MoSe_2$ sample.

T1.3 Synthesis and optical properties of large-scale single-crystalline two-dimensional semiconductor WS_2 monolayer from chemical vapor deposition

Chunxiao Cong, Ting Yu

Wednesday, February 26, 02.30 PM, Rooms 1+2

Two-dimensional (2D) transition metal dichalcogenides (TMDs), especially MoS_2 and WS_2 recently attract extensive attentions due to their rich physics and great potential applications. Superior to graphene, MS_2 (M = Mo/W) monolayers have a native direct energy gap in visible frequency range. This promises great future of MS_2 for optoelectronics. To exploit properties and further develop more applications, producing large-scale single crystals of MS_2 by a facile method is highly demanded. Here, we report our study of growing large-scale triangular single crystals of WS_2 monolayer up to hundreds of microns by one step of direct sulfurization of WO3 powders and probing their optical properties. The observations of high yield of light emission and valley-selective circular dichroism experimentally evidence the high optical quality of the WS_2 monolayers. This work paves the road to fabricate large-scale single crystalline 2D semiconductors and study their fundamentals. It must be very meaningful for exploiting great potentials of WS_2 for future optoelectronics.

T1.4 A study of sub-ten femtosecond carrier relaxation in single layer graphene using z-scan

David Giovanni

Wednesday, February 26, 02.50 PM, Rooms 1+2

Graphene is a single atom thick class of layered material which holds great potential for future applications in spintronic, valleytronic, etc. - attributable to its exotic gapless linear band structure in spectral regime below 3 eV. However, complete understanding of the carrier relaxation mediated by carrier-carrier (c-c) scattering within time regime of 10 fs post-excitation has never been achieved yet, due to the limitation of current laser's temporal pulse width used in pump-probe setup. This study therefore attempts construct a theoretical model which is integrated to the open-aperture z-scan technique. Relaxation time of a process much shorter than the temporal pulse width of a femtosecond laser can be elucidated using this approach. This new technique is then applied to investigate the relaxation process mediated by carrier-carrier scattering in single layer

graphene. Under low pump fluence, our findings yields a lifetime of 9 fs, which is consistent with previous study. At high pump fluence, our findings uncovered an Auger-type c-c scattering process that quenches the lifetimes to a saturated value of 4 fs. The origin of the Auger type scattering process is attributed to the modification of quasiparticle band structure and anisotropic linear excitation under high pump fluence.

6.2 T2 Bubbles and cavitation

This session will be held on Wednesday, February 26, from 01.30 PM to 03.00 PM. Venue for this session is Rooms 3+4. Time allocated for invited talks is 25 min speaking time, plus 5 min Q&A, and time allocated for contributed talks is 15 min speaking time plus 5 minutes Q&A.

T2.1 Modeling and simulation of an elastic object near an oscillating bubble using the Boundary Element Method (INVITED)

Siew-Wan Ohl, Tandiono Tandiono, Evert Klaseboer, Fenfang Li, Claus-Dieter Ohl

Wednesday, February 26, 01.30 PM, Rooms 3+4

The study of bubble dynamics using the Boundary Element Method has been done extensively [1-3]. It is known that when an oscillating bubble collapses near a rigid boundary it would jet towards the boundary; near a free boundary, it would jet away. The interaction of a bubble near an elastic interface is more complicated. Brujan et al. [4, 5] generated a laser-induced bubble near a polyacrylamide (PAA) gel. They varied the elasticity of the gel by modifying the water content of the gel. The observations from the high speed photography showed that complex bubble dynamics such as a 'mushroom-shaped' bubble, bubble splitting, and bubble jetting. Numerical simulations which compares with experiments using a spark generated bubble by Turangan et al [6] demonstrated the detailed mechanics behind the interactions. Recent article by Gong et al [7] showed similar complicated interaction between an explosion bubble and composite beam. The simulation in [7] is done using a combined code of Boundary Element and a Finite Element solver (PAMCrash). Another group experimented the interaction of a laser-induced bubble near a group of Red Blood Cells (RBC) [8]. They could extract the elastic properties of the cells from the high speed experimental observations. We found that the Boundary Element Method is capable of modeling the stretching of the RBC by considering the cells as an elastic object with surface tension [9]. We observe that the stretching can only occur if the cell exhibits some elastic properties within a certain threshold. The maximum elongation occurs when the oscillations of the bubble and cell are out of phase, that is, the bubble oscillates at half the oscillation time of the cell.

Reference: [1] Blake, J. R., & Gibson, D. C. (1987). Cavitation bubbles near boundaries. Annual Review of Fluid Mechanics,19(1), 99-123; [2] Wang, Q. X., Yeo, K. S., Khoo, B. C., & Lam, K. Y. (1996). Nonlinear interaction between gas bubble and free surface. Computers & Fluids, 25(7), 607-628; [3] Klaseboer, E., Hung, K. C., Wang, C., Wang, C. W., Khoo, B. C., Boyce, P., Debono, S., & Charlier, H. (2005). Experimental and numerical investigation of the dynamics of an underwater explosion bubble near a resilient/rigid structure. Journal of Fluid Mechanics,537, 387-413; [4] Brujan, E. A., Nahen, K., Schmidt, P., & Vogel, A. (2001). Dynamics of laser-induced cavitation bubbles near an elastic boundary. Journal of Fluid Mechanics, 433, 251-281; [5] Brujan, E. A., Nahen, K., Schmidt, P., & Vogel, A. (2001). Dynamics of laser-induced cavitation bubbles near elastic boundaries: influence of the elastic modulus. Journal of Fluid Mechanics, 433, 283-314; [6] Turangan, C.K., Ong, G.P., Klaseboer, E. & Khoo, B.C. 2006 Experimental and numerical study of transient bubble-elastic membrane interaction. J.

Appl. Phys. 100, 054910; [7] Gong, S. W., Ohl, S. W., Klaseboer, E., & Khoo, B. C. (2010). Scaling law for bubbles induced by different external sources: Theoretical and experimental study. Physical Review E, 81(5), 056317; [8] Quinto-Su, P. A., Kuss, C., Preiser, P. R., & Ohl, C. D. (2011). Red blood cell rheology using single controlled laser-induced cavitation bubbles. Lab on a Chip,11(4), 672-678; [9] Tandiono, T., Klaseboer, E., Ohl, S. W., Ow, D. S. W., Choo, A. B. H., Li, F., & Ohl, C. D. (2013). Resonant stretching of cells and other elastic objects from transient cavitation. Soft Matter, 9(36), 8687-8696.

T2.2 Petals and fractals: how soap bubbles merge

Beng Hau Tan, Robin van de Vondervoort, Silvestre Roberto Gonzalez-Avila, Rogerio Manica, Evert Klaseboer, Claus-Dieter Ohl

Wednesday, February 26, 02.00 PM, Rooms 3+4

The merging of two soap bubbles is the fundamental process in foam formation. Understanding such processes is crucial, as foams are widely utilized in life-science and industrial applications. Experimentally we study with high-speed photography the contact region when two soap bubbles merge. As the process is rapid, framing rates of 100,000 frames per second are necessary. For simple solutions of water, thickener, and surfactant we observe that a circular contact plane is formed and its radius grows at a constant velocity. As the merger proceeds, the column of liquid is experimentally observed to thin considerably. Numerical simulations support this picture and suggest that the contact between the two soap bubbles is initiated when once a liquid bridge is formed. Interestingly, commercial bubble solutions often additionally contain long-chained detergents. These complex liquids give rise to beautiful dynamic structures formed during the coalescence, such as petals and even self-repeating, fractal-like projections.

T2.3 Dynamics and stability of nanobubbles inside the Transmission Electron Microscope (TEM)

Meera Kanakamma Mohan, Manish Arora, Utkur Mirasaidov, Claus-Dieter Ohl

Wednesday, February 26, 02.20 PM, Rooms 3+4

Liquid cell electron microscopy is a novel technique for imaging liquids with high spatial resolution inside the transmission electron microscope (TEM). Here we report on the bubble dynamics in water trapped between two monolayers of graphene sheets supported by a conventional TEM grid. The graphene liquid cell geometry provides excellent electron-optical properties for investigations and prevents the evaporation of liquid into the low pressure environment of the TEM. We report on various bubble dynamics, including coalescence of neighbouring bubbles, thin liquid film rupture and slow shrinkage of bubbles. At a dose rate of 100-155 $e^-/\text{Å}^2/\text{s}$, the dynamics are conveniently observed at video frame rate. The lateral size of the bubbles is in between 20 nm to 100 nm and the height varies from 6 nm to 30 nm. The bubbles are likely to attach both graphene sheets. We observed that the nanobubbles do not dissolve completely in the absence of the beam, but remain stable for hours. This observation resembles the 'mysterious' stability of surface attached nanobubbles.

T2.4 Interaction of a laser induced cavitation bubble with complex configurations of gas-bubbles

Fenfang Li, Evert Klaseboer, Manish Arora, Claus Dieter Ohl

Wednesday, February 26, 02.40 PM, Rooms 3+4

Introduction

Shockwave-gas bubbles interaction may lead to very intense flow. One of the concerns is the haemolysis of red blood cells in shock wave lithotripsy due to the flow created by impulsively collapsing bubbles. Here we present a technique to study this interaction in a controlled manner using microfluidic confinement.

Materials and Methods

Single or multiple micron-size gas bubble(s) are generated in water confined in a microfluidic gap by heating a gold coated substrate with a continuous laser beam. The position and size of the gas bubbles are defined by a digital hologram and the duration of the laser exposure, respectively. Additionally, a pulsed laser is focused in the liquid to generate a rapidly expanding cavitation bubble next to the gas bubble(s). The dynamics is recorded using high speed photography with frame rate of more than 1 million frames/s.

Results and Conclusion

For single gas bubble, the impulsive acceleration of the liquid causes an asymmetric collapse with the formation of a fast jet (with the averaged velocity more than 120 m/s) away from the cavitation bubble. Later the cavitation bubble collapses and re-expands. This abrupt motion compresses the gas bubble for second time. By varying the size of the cavitation bubble, size of the gas bubble as well as distance between both, different jetting patterns are observed during the collapse. Interestingly, fast expansion of the cavitation bubble leaves a liquid film on the surface. This liquid film is ruptured when the cavitation bubble expands over the original site of the gas bubble.

The setup allows to generate complex gas bubble configurations. When an array of gas bubbles is exposed to the laser induced cavitation bubble, the gas bubbles undergo simultaneous or cascaded collapses depending on their geometric arrangement.

The experiments mimic the classical experiments from Dear & Field on millimetre-size 2D bubbles in gelatine. Yet, our technique allows the easy generation of arbitrary gas bubble geometries on a scale relevant for biology. We have already applied single cavitation induced jets for membrane rupture and drug injection into biological cells. Further we hope to present at the conference first results on enhancing haemolysis.

6.3 T3 Quantum Information 1

This session will be held on Wednesday, February 26, from 01.30 PM to 03.00 PM. Venue for this session is Rooms 5+6. Time allocated for invited talks is 25 min speaking time, plus 5 min Q&A, and time allocated for contributed talks is 15 min speaking time plus 5 minutes Q&A.

T3.1 An information-theoretic principle implies that any discrete physical theory is classical (INVITED)

Corsin Pfister, Stephanie Wehner

Wednesday, February 26, 01.30 PM, Rooms 5+6

It has been suggested that nature could be discrete in the sense that the underlying state space of a physical system has only a finite number of pure states. Here we present a strong physical argument for the quantum theoretical property that every state space has infinitely many pure states. We propose a simple physical postulate that dictates that the only possible discrete theory is classical theory. More specifically, we postulate that no information gain implies no disturbance or, read in the contrapositive, that disturbance leads to some form of information gain. Furthermore, we show that non-classical discrete theories are still ruled out even if we relax the postulate to hold only approximately in the sense that no information gain only causes a small amount of disturbance. Our postulate also rules out popular generalizations such as the Popescu–Rohrlich-box that allows non-local correlations beyond the limits of quantum theory.

Nature Communications publication: http://www.nature.com/ncomms/journal/v4/n5/full/ncomms2821
arXiv version: http://arxiv.org/abs/1210.0194

T3.2 Entropic formulation of Heisenberg's measurement-disturbance relation

Patrick Coles, Fabian Furrer

Wednesday, February 26, 02.00 PM, Rooms 5+6

Heisenberg's original intuition was that there should be a tradeoff between measuring a particle's position with greater precision and disturbing its momentum. Rigorous formulations of this idea have primarily focused on the question of how well two complementary observables can be jointly measured. Here, we provide an alternative approach based on how enhancing the predictability of one observable necessarily disturbs a complementary one. The tradeoff refers to a clear operational scenario capturing the effect of the measurement process on a single quantum system. Moreover, our relation is expressed by entropic quantities with clear statistical meaning evading recent criticism directed at some previous formulations. We discuss the performance of our tradeoff relation for existing experimental setups involving qubit measurements performed in Vienna and Toronto, and show that our relation is perfectly tight for all measurement strengths in the Toronto setup.

T3.3 Randomness extraction from quantum systems with different levels of trust in the working of the devices

Yun Zhi Law, Jean-Daniel Bancal, Valerio Scarani

Wednesday, February 26, 02.20 PM, Rooms 5+6

The amount of intrinsic randomness that can be extracted from measurement on quantum systems depends on several factors: in this paper we compare various levels of trust in the working of the devices of the authorized partners. Many recent studies have focused the so-called "device-indepependent" level: by violating a Bell inequality, a lower bound on the amount of randomness present in the data can be certified without knowing any operational details about the devices. When on the contrary all the devices are trusted, specific measurements can be chosen in order to extract the maximal amount of randomness. This "tomographic" level of trust is well known (in a sense, it has been known since people noticed that there is randomness in quantum physics); but we present a systematic approach to quantifying the amount of extractable randomness. Finally, we introduce an intermediate level of trust, related to the task of "steering", in which the device of one party is trusted but not the other's.

T3.4 Strong Parallel Repetition for a Monogamy-of-Entanglement Game

Marco Tomamichel, Serge Fehr, Jedrzej Kaniewski, Stephanie Wehner

Wednesday, February 26, 02.40 PM, Rooms 5+6

Apart from their obvious entertainment value, games among multiple (competing) players often provide an intuitive way to understand complex problems. For example, we may understand Bell inequalities in physics, or interactive proofs in computer science, as a game played by a referee against multiple provers. Here we investigate a simple quantum multiplayer game whose analysis enables us to tackle several open questions in quantum cryptography.

6.4 T4 Plasma Physics

This session will be held on Wednesday, February 26, from 03.30 PM to 05.10 PM. Venue for this session is Rooms 1+2. Time allocated for invited talks is 25 min speaking time, plus 5 min Q&A, and time allocated for contributed talks is 15 min speaking time plus 5 minutes Q&A.

T4.1 Generation of Strong Half-cycle THz Radiation with Ultrashort Laser (INVITED)

Wen Jun Ding, Wee Shing Koh, Zheng Ming Sheng

Wednesday, February 26, 03.30 PM, Rooms 1+2

Terahertz (THz) radiation provides wide applications in non-invasive imaging, information, security and fundamental science. Although the well-known "THz-gap" has begun to be filled through advances in many areas, much of its potential still remains untouched. One reason is the lack of high-intensity of THz sources. Here, we found that half cycle THz radiations with peak field over 100MV/cm can be produced by ultrashort laser-solid interactions. The THz pulses are emitted in both forward and backward directions from the front and rear side of the target respectively. The emissions are attributed to coherent transition radiation when hot electrons transmit through the vacuum-target interfaces. After the primary THz pulses, subsequent secondary pulses are generated due to some refluxing electrons crossing the surfaces. Our scheme offers a route to produce ultra-strong THz sources, and also provides a unique way to understand the transport of electron beam in a dense plasma target.

T4.2 Plasma Focus: Small and Cost-effective Fusion Device for Plasma/Nuclear Research and Training (INVITED)

Rajdeep Singh Rawat

Wednesday, February 26, 04.00 PM, Rooms 1+2

Milestone nuclear fusion facilities, such as ITER based on magnetic and NIF based on inertial plasma confinement concepts, are currently under construction or in operation aiming at demonstrating ignition and energy gain. While the mainstream nuclear fusion research is currently being undertaken in many big fusion machines such as JET, LHD, JT-60, LMJ, Z, K-Star, NIF etc. however much to the science and technology of nuclear fusion has come through the research done on laboratory size fusion experiments on medium size and small scale tokamaks, compact tori, dense plasma focus, reversed field pinches, helical devices, linear machines, and other small plasma devices. The big fusion devices need years of planning and huge financing but small fusion devices can be built and operate as moderate cost. Hence small fusion devices are ideal workbench for emerging economies or the countries which are new to the plasma/nuclear/fusion research. NIE's high energy density plasma research team at Plasma Radiation Source Lab is a global leader in low and medium energy single-shot high repetition-rate dense plasma focus device research. Our research spans fundamental plasma, nuclear fusion and radiation science and diagnostics as well as applications in various fields such as:

neutron source for novel material testing for first wall of fusion reactor, radioisotopes synthesis, soft X-ray lithography, soft and hard X-ray imaging, material modification, and nano-structured material synthesis. The team has successfully delivered and established plasma focus devices at Imperial College (London, UK), Kansas State University (USA), Technological Educational Institute of Crete (Greece) and INTI International University (Malaysia) which firmly establish their global leadership position in this field. This paper will discuss the avenues and opportunities provided by a small fusion device called plasma focus in the field of science, technology and applications of plasma, nuclear and fusion research, such as: (i) transport, turbulence, confinement and stability of fusion plasmas, (ii) characterization of energetic charged particles (ions and electron beam), energetic photons (soft and hard x-rays) and fusion neutrons, (iii) technology developments such as new neutron, charged particles and radiation diagnostic concepts and prototypes, and (iv) novel material synthesis and plasma facing materials testing as well as characterization and improvement.

T4.3 Plasma flares and ion acceleration in high power impulse magnetron sputtering

Joakim Andersson, Matjaž Panjan, Robert Franz, Pavel Ni, André Anders

Wednesday, February 26, 04.30 PM, Rooms 1+2

Recent investigations of high power impulse magnetron sputtering discharges have revealed inhomogeneities in the form of traveling ionization zones resulting in plasma flares. Such plasma structures affect the spatial distribution of the kinetic energy of sputtered ionized atoms, and are therefore important for the growth and quality of the deposited film. Short exposure images of plasma inhomogeneities of aluminium atoms and ions as well as argon atoms and ions will be presented. Analysis of these images together with ion kinetic energy determination has led to an explanation of the tangential (E $\times$ B) acceleration and deceleration of ions previously reported by other authors. We show that azimuthally traveling ionization zones are associated with electrostatic 'potential humps' preferentially accelerating ions in the direction of ionization zone movement.

T4.4 CHALLENGES AND PROSPECTS IN THE REALIZATION OF MINIATURE PLASMA FOCUS DEVICE AS A SOFT X-RAY LITHOGRAPHY SOURCE

S. M. P. Kalaiselvi, Tuck Lee Tan, Alireza Talebitaher, Paul Lee, Rajdeep Singh Rawat

Wednesday, February 26, 04.50 PM, Rooms 1+2

Plasma based emission is a complex phenomenon, which when harnessed effectively can be a rich source of high energy radiations and particles. Plasma and the type of dominant emission from it can be determined through tuning of electrical circuit parameters and the parameters of the filling gas. Furthermore, the dominant emission can be enhanced through doping of high-Z impurity ions at the right proportion to the operating gas. While, the enhanced emission of specific radiation is possible from the plasma focus device, slight deviation from optimized parameters can lead to very poor performance of the device accompanied by uncertainty in the identification of the source of the poor performance. Optical investigations such as time integrated imaging of the plasma focus

dynamics using laser Shadowgraphy, time resolved imaging of the fast moving plasma using a high speed gated ICCD camera, together with monitoring of performance of pseudo spark gap switches using magnetic pick up loops and current derivative signal using Rogowski coil were done, to understand the influence of various circuit parameters and the parameters of the filling gas on the soft X-ray emission efficiency of the device.

6.5 T5 Topological Insulators 1

This session will be held on Wednesday, February 26, from 03.30 PM to 05.00 PM. Venue for this session is Rooms 3+4. Time allocated for invited talks is 25 min speaking time, plus 5 min Q&A, and time allocated for contributed talks is 15 min speaking time plus 5 minutes Q&A.

T5.1 Detecting symmetry protected topological phases in low dimensions

Keola Wierschem, Pinaki Sengupta

Wednesday, February 26, 03.30 PM, Rooms 3+4

Symmetry protected topological phases possess edge states that are protected from local perturbations preserving select symmetries. One example of such a phase is the Haldane gap phase of spin S=1 Heisenberg chains. In this case, the edge states are spin-1/2 degrees of freedom that are protected by any of the symmetries time reversal, space inversion, or O(3) spin rotation. While the Haldane gap phase does not break any Hamiltonian symmetry, there exists a unitary transformation under which it breaks an emergent Z2×Z2 symmetry – so called hidden symmetry breaking. The local order parameter for this symmetry breaking, when transformed back to the original Hamiltonian system, becomes the non-local order parameter – so called string order. Here, we study string order in antiferromagnetic spin-1 Heisenberg chains with single-ion anisotropy as well as weakly coupled chains in higher dimension.

T5.2 Network models of photonic Floquet topological insulators (INVITED)

Michael Pasek, Yidong Chong

Wednesday, February 26, 03.50 PM, Rooms 3+4

Drawing inspiration from the network model picture of the localization-delocalization transition in Quantum Hall systems, and the recent works on dynamically induced topological phases of condensed matter, we show how to construct two-dimensional photonic lattices ("photonic networks") that display topologically protected "one-way" edge states. We demonstrate how the bulk-edge correspondence in those systems can be understood from Floquet analysis, why such networks can display "anomalous" adiabatic pumping properties, and how one would go about probing the topological states in the lab by measuring the reflection matrix off one edge of the network.

T5.3 Ultrafast Dynamics of $Bi_{1.5}Sb_{0.5}Te_{1.8}Se_{1.2}$ Topological Insulator

Liang Cheng, Chan La-O-Vorakiat, Chi Sin Tang, Saritha K. Nair, Bin Xia, Lan Wang, Jian-Xin Zhu, Elbert E. M. Chia

Wednesday, February 26, 04.20 PM, Rooms 3+4

$Bi_{1.5}Sb_{0.5}Te_{1.8}Se_{1.2}$ (BSTS) is a type of topological insulator, which is an insulator in bulk but surface states are gapless [1, 2]. In this work, we took optical pump-probe data on BSTS crystal to analyze the dynamics of phonons and charge carriers. The ultrafast dynamics were obtained as a function of temperature ranging from 10 K to 300 K, as well as fluence ranging from 1 µJ/cm^2 to 10 µJ/cm^2. In additional to the coherent optical

phonon mode found in other topological insulators [3, 4], acoustic phonon mode was observed in our experiment. We also observed phonon softening and the temperature dependence of carrier lifetime in BSTS.

References: [1] J. E. Moore, Nature 464, 194 (2010); [2] M. Z. Hasan et. al. Rev. Mod. Phys. 82, 3045 (2010); [3] Y. W. Li et. al. Appl. Phys. Lett. 97, 171908 (2010). [4] N. Kumar et. al. Phys. Rev. B 83,235306 (2011).

T5.4 Optical Properties of Topological Insulator

Zilong Wang, Jun Yin, Giorgio Adamo, Venkatram Nalla, Stefano Vezzoli, Azat Sulaev, Lan Wang, Handong Sun, Nikolay I. Zheludev, Cesare Soci

Wednesday, February 26, 04.40 PM, Rooms 3+4

We report on optical properties of chalcogenide crystal of the Bi-Sb-Te-Se family that was recently identified as a prospective platform for switchable broadband plasmonic devices. The electronic bandgap energy and dielectric functions are obtained by first-principle density functional theory (DFT) and compared to the results of low-temperature transmittance and reflectance spectra, showing two regions of anomalous dispersion due to the combination of bulk interband transitions and surface contribution of the topologically protected states in the UV and the bandgap region (5 µm). Steady-state and femtosecond transient absorption upon photoexcitation with visible light show the potential of topological insulators for broadband, high-frequency switchable metamaterials.

6.6 T6 Quantum Information 2

This session will be held on Wednesday, February 26, from 03.30 PM to 05.00 PM. Venue for this session is Rooms 5+6. Time allocated for invited talks is 25 min speaking time, plus 5 min Q&A, and time allocated for contributed talks is 15 min speaking time plus 5 minutes Q&A.

T6.1 Entangled quantum states without multipartite correlations (INVITED)

Minh Tran, Tomasz Paterek

Wednesday, February 26, 03.30 PM, Rooms 5+6

All entangled bipartite quantum states are correlated. However, extrapolation to the multipartite case does not hold. We first show theoretically that it is always possible to erase correlations between an odd number of qubits, while this is not possible between an even number of them. This allows us to construct an infinite family of states that exhibit genuine tripartite entanglement without tripartite correlations. We then develop experimentally friendly criterion in order to detect this entanglement and perform experiments demonstrating entanglement without correlations in polarisation entangled three photon mixed states.

T6.2 Optimal Error Regions for Quantum State Estimation

Hui Khoon Ng, Jiangwei Shang, Yi-Lin Seah, Xikun Li, David Nott, Berthold-Georg Englert

Wednesday, February 26, 04.00 PM, Rooms 5+6

Quantum state estimation is a crucial primitive underlying a multitude of quantum information processing tasks. A good estimation strategy requires not only an accurate guess with minimal amount of data, but also a statement about how certain we are of our guess. To this end, we previously introduced [New J. Phys. 15, 123026 (2013)] the notion of optimal error regions, where a region in state space, rather than a single point, is given to encapsulate the certainty—in terms of the Bayesian notion of credibility—of our guess, and optimality is quantified by a region of smallest size for the given level of credibility. These optimal error regions turn out to have very simple and elegant characterization, and bear close similarity to error regions from traditional statistical analysis applicable only to large data-sets (yet, our analysis requires no such assumption); a surprising independence of the choice of prior also emerged from our analysis. Here, we report on our recent progress in efficient computation of these optimal error regions, discuss more examples, as well as extend the notion to include parameter estimation tasks.

T6.3 Separable states improve protocols with restricted randomness

Bobby Tan, Tomasz Paterek

Wednesday, February 26, 04.20 PM, Rooms 5+6

We present general arguments that separable states constitute a useful resource whenever randomness is not free. In particular, it is shown that they improve correlation assisted random access codes where correlated classical bits are replaced with correlated

qubits. We show how the bias of classical bits can be used to avoid wrong answers and how advantage of quantum protocols is linked to quantum discord.

T6.4 Self-Stabilizing Measurement of Phase

Sai Vinjanampathy

Wednesday, February 26, 04.40 PM, Rooms 5+6

Measuring phase accurately constitutes one of the most important task in precision measurement science. Such measurements can be deployed to measure everything from fundamental constants to measuring detuning and tunneling rates of atoms more precisely. Quantum mechanics enhances the ultimate bounds on the precision of such measurements possible, and exploit coherence and entanglement to reduce the phase uncertainty. In this work, we will describe a method to stabilize a decohering two-level atom and use the stabilizing measurements to learn the unknown phase acquired by the atom. Such measurements will employ a Bayesian learner to do active feedback control on the atom. We will discuss some ultimate bounds employed in precision metrology and an experimental proposal for the implementation of this scheme.

6.7 T7 Topological Insulators 2

This session will be held on Thursday, February 27, from 01.30 PM to 03.10 PM. Venue for this session is Rooms 1+2. Time allocated for invited talks is 25 min speaking time, plus 5 min Q&A, and time allocated for contributed talks is 15 min speaking time plus 5 minutes Q&A.

T7.1 Gated Quantum Transport in topological insulator BiSbTeSe and beta-Ag2Te (INVITED)

Azat Sulaev, Lei Shen, Bin Xia, Shun-Qing Shen, Kie Leong Teo, Wei Guang Zhu, Yuan Ping Feng, Ming Yong Han, Ting Yu, Lan Wang

Thursday, February 27, 01.30 PM, Rooms 1+2

We present our recent work of gated quantum transport in topological insulator BiSbTeSe and beta-Ag2Te. For BiSbTeSe system: We report experimental evidence of surface dominated transport in single crystalline nanoflake devices of topological insulator Bi1.5Sb0.5Te1.8Se1.2. Based on a two-channel model, the analysis on the resistivity and Hall resistance indicates that 99

For beta-Ag2Te system: We observed the coexistence of pronounced Aharonov-Bohm oscillations and weak Altshuler-Aronov-Spivak oscillations clearly demonstrates coherent electron transport around the perimeter of beta-Ag2Te nanoribbon and therefore the existence of surface states, We also report the first experimental confirmation of the existence of topological surface states with large electric field tunability and mobility in beta-Ag2Te. Pronounced 2D SdH oscillations have been observed in both beta-Ag2Te nanoplate and nanowire. A Berry phase is determined to be near pi using the Landau level fan diagram for nanoplate while the largest electric field ambipolar effect in topological insulator so far (≈2500

T7.2 Phonon dispersion relations of Sb2S3 and Bi2S3 using the supercell force-constant method (INVITED)

Chee Kwan Gan, Kunting Chua, Yun Liu

Thursday, February 27, 02.00 PM, Rooms 1+2

We present a lattice dynamical study on the orthorhombic antimony sulphide (Sb2S3) [1] and bismuth sulphide (Bi2S3) [2] using the supercell force-constant method. We find that the slow decay of the interatomic force constants for these compounds in the Pnma setting requires the use of a large supercell of 2 x 4 x 2 that consists of 320 atoms. To enable a practical calculation the space group information is fully utilized where only inequivalent atoms within the primitive cell are displaced for the force calculations. The effect of Born effective charges is incorporated into the method. We compare our results with that obtained from the density-functional perturbation theory. We found that smaller supercells could lead to unphysical acoustic phonon softening and lifting of the degeneracies along high symmetry directions. Our results serve to suggest that

for a proper use of the supercell force-constant method, the supercell size has to be tested along with other parameters such as the kinetic energy cutoff, the Brillouin zone sampling or the self-consistent convergence criteria.

[1] Y.Liu, K.T.E. Chua, T.C. Sum, and C.K. Gan, PCCP 16 (2014) 345. [2] Y. Zhao, K.T.E. Chua, C.K. Gan, J. Zhang, B. Peng, Z. Peng, and Q. Xiong, Phys. Rev. B 84 (2011) 205330.

T7.3 Terahertz conductivity of topological surface states in $Bi_{1.5}Sb_{0.5}Te_{1.8}Se_{1.8}$

Chi Sin Tang, Bin Xia, Xingquan Zou, Shi Chen, Hong-Wei Ou, Lan Wang, Andrivo Rusydi, Jian-Xin Zhu, Elbert E. M. Chia

Thursday, February 27, 02.30 PM, Rooms 1+2

Topological insulators are electronic materials with an insulating bulk and conducting surface. However,due to free carriers in the bulk, the properties of the metallic surface are difficult to detect and characterize in most topological insulator materials. Recently, a new topological insulator $Bi_{1.5}Sb_{0.5}Te_{1.8}Se_{1.8}$ (BSTS) was found, showing high bulk resistivities of 1–10 Ω.cm and greater contrast between the bulk and surface resistivities compared to other Bi-based topological insulators. Using Terahertz Time-Domain Spectroscopy (THz-TDS), we present complex conductivity of BSTS single crystals, disentangling the surface and bulk contributions. We find that the Drude spectral weight is 1–2 orders of magnitude smaller than in other Bi-based topological insulators, and similar to that of Bi2Se3 thin films, suggesting a significant contribution of the topological surface states to the conductivity of the BSTS sample. Moreover, an impurity band is present about 30 meV below the Fermi level, and the surface and bulk carrier densities agree with those obtained from transport data. Furthermore, from the surface Drude contribution, we obtain a ,98

T7.4 Bulk effects on topological conduction in 3-D topological insulators

Vincent Sacksteder, Quansheng Wu

Thursday, February 27, 02.50 PM, Rooms 1+2

The surface states of a topological insulator in a fine-tuned magnetic field are ideal candidates for realizing a topological metal which is protected against disorder. Its signatures are (1) a conductance plateau in long wires and (2) an always-increasing conductivity, and are independent of disorder strength and sample size. We numerically study how these transport signatures are affected by bulk physics in the interior of the topological insulator sample. We show that both signatures of the topological metal are robust against bulk effects. However the bulk does substantially accelerate the metal's decay in a magnetic field and alter its response to surface disorder. When the disorder strength is tuned to resonance with the bulk band the conductivity follows the predictions of scaling theory, indicating that conduction is diffusive. At other disorder strengths scaling theory is systematically violated, signaling that scattering is reduced and the topological metal is not fully diffusive.

6.8 T8 Lasers

This session will be held on Thursday, February 27, from 01.30 PM to 03.10 PM. Venue for this session is Rooms 3+4. Time allocated for invited talks is 25 min speaking time, plus 5 min Q&A, and time allocated for contributed talks is 15 min speaking time plus 5 minutes Q&A.

T8.1 Microlaser goes to flexible (INVITED)

Van Duong Ta, Rui Chen, Handong Sun

Thursday, February 27, 01.30 PM, Rooms 3+4

We demonstrate the feasibility of constructing flexible high Q-factor solid state microcavities. The configurations of the microresonators include hemispheres, fibres, and whole sphere droplets. We have clearly observed optically pumped lasing from these structures. The lasing characteristics have been systematically investigated in terms of size dependence, temperature dependence and polarization. Especially we have shown that some structures can be operated at single and tunable-frequency. Finally very sensitive refractive index sensing can be conveniently realized from these structures.

T8.2 THz lasing from dipolaritons (INVITED)

Kristinn Kristinsson, Oleksandr Kyriienko, Ivan Shelykh, Tim C. H. Liew, Alexei Kavokin

Thursday, February 27, 02.00 PM, Rooms 3+4

Generation of continuous terahertz (THz) radiation remains an important physical challenge, with free-electron lasers and QCLs suffering from bulky size and cryogenic operating temperature respectively. Here we present a scheme for generating THz lasing in a dipolariton system, consisting of a microcavity with embedded double quantum wells. In this system direct and indirect excitonic modes couple linearly with each other and the cavity mode, and the new light-matter eigenmodes are called upper, middle and lower polaritons. We show that pulsed excitation of the system results in oscillatory relaxation of the direct and indirect exciton occupation numbers. Indirect excitons carry a dipole moment, and oscillations correspond to an array of classical dipole antennae, which emit radiation in the THz range. By accounting for interexciton interactions we describe multistabilities under optical continuous wave (CW) pumping. Furthermore, we find conditions of parametric instability, resulting in indirect exciton number oscillations under CW pumping. By embedding the system in a THz optical cavity tuned to the frequency of these oscillations, we demonstrate THz frequency lasing. Analysing the dependence of the output power on THz cavity quality factor, we show that a relatively low (15-30) value is optimal. Additionally we demonstrate superradiance of the system, that the emission power depends superlinearly on the system size. This allows for high emission power at the engineering stage by up-scaling of the device, making the system competitive with other schemes of THz generation.

T8.3 S-matrix Theory of the Laser Linewidth

Yidong Chong, Jason Pillay

Thursday, February 27, 02.30 PM, Rooms 3+4

We present a theoretical relation between the classical scattering matrix (S-matrix) of a spatially complex optical cavity and the quantum-limited laser linewidth. This theory is an advance over previous theoretical approaches to the laser linewidth, in that it can account for arbitrary cavity geometries, spatially non-uniform dielectric and gain distributions, and spatial hole-burning due to above-threshold operation. In simple 1D Fabry Perot cavities, the Schawlow-Townes linewidth formula is reproduced, together several well-known corrections such as the Petermann factor. We also derive a novel geometric explanation for the Petermann and bad-cavity factors, which act to increase and decrease the laser linewidth respectively. Although previous theories have treated these as independent quantities, we show that this independence assumption breaks down in complex laser cavities when line-pulling is non-negligible. The S-matrix theory may thus be useful for studying complex lasers with narrow gain widths, such as superradiant lasers.

T8.4 Integration of a III-V nanowire in a Silicon Nitride photonic crystal

Christophe Wilhelm, Sylvain Combrie, Gaelle Lehoucq, Alfredo De Rossi, Cesare Soci

Thursday, February 27, 02.50 PM, Rooms 3+4

In the past decade, there has been an increasing interest in the study of photonic devices as future elements for increasing data transfer speeds in intra-chip intercommunications. In particular, photonic crystal membranes have proven to be useful tools for optical communications as they allow sub-wavelength control over the light flow, thus allowing miniaturization and all-on-chip operations. Several building blocks have already been shown (e.g. filters, waveguides, and others), however an integrated, on-chip light source is still lacking. Thanks to their opto-electronic properties, semiconductor nanowires of the III-V group have tremendous potential for the development of future photonic devices. Their high aspect ratio and high index of refraction makes nanowires a natural fabry-perot like cavity, where the constituent semiconductor crystal can serve as gain medium. Indeed, stimulated emission has been reported in various nanowire materials, despite the significant losses in the host substrate. Here, we propose a novel structure towards the achievement of integrated, on-chip light sources combining these two technologies. The III-V nanowire buried in a silicon nitride photonic crystal membrane will act as a gain medium, using the photonic crystal light confinement properties to reduce the losses. We will present electromagnetic simulations of the proposed structure for the design of suitable photonic crystal membranes, as well as the first fabrication attempt of such structures.

6.9 T9 Atomic and Molecular Physics

This session will be held on Thursday, February 27, from 01.30 PM to 02.40 PM. Venue for this session is Rooms 5+6. Time allocated for invited talks is 25 min speaking time, plus 5 min Q&A, and time allocated for contributed talks is 15 min speaking time plus 5 minutes Q&A.

T9.1 Coherent transmission through a cold atomic gas (INVITED)

Chang Chi Kwong, David Wilkowski, Dominique Delande, Romain Pierrat

Thursday, February 27, 01.30 PM, Rooms 5+6

We studied theoretically and numerically various effects in the coherent forward transmission of a probe beam through a cloud of cold atomic gas. We investigated the forward coherent transmission both in the stationary and transient regimes. In the stationary regime, we calculated the second order correction in density to the relative permittivity of the atomic cloud. This allows the computation of the stationary state attenuation and the phase shift of the coherently transmitted beam in a non-dilute atomic cloud. In the transient regime, a coherent flash with initial transmission close to 1 can be observed after an abrupt extinction of the probe beam incident on a cold strontium-88 cloud [1]. We theoretically predicted and numerically validated the conditions required to observe a "superflash" with an initial transmission greater than 1. This is physically possible due to the storage of energy in the excited levels of the atomic gas. Our laboratory are currently working towards experimentally verifying the above predictions.

[1] M. Chalony and R. Pierrat and D. Delande and D. Wilkowski, Phys. Rev. A 84, 011401(R) (2011).

T9.2 Atom interferometry with guided matter waves in optical fibers

Shau-Yu Lan

Thursday, February 27, 02.00 PM, Rooms 5+6

Precision measurement with light-pulse grating atom interferometry in free space have been used in the study of fundamental physics, such as measuring fine structure constant, testing general relativity, and building a clock referenced the mass of a single particle. It also finds its applications in gravimetry, gradiometry, and rotation sensing. However, due to the diffraction nature of light, this approach requires large-diameter laser beams to maximize its sensitivity while minimizing systematic effect and therefore complex the experimental setup. Recent development of photonic bandgap fibers allows light for travelling in hollow region while preserving its fundamental Gaussian mode. Optically guided matter waves inside a hollow-core photonic bandgap fiber can mitigate this diffraction limit problem and has the potential to bring research in the field of atomic sensing and precision measurement to the next level of compactness and accuracy. Here, I will give an overview of precision atom interferometry and have discussion on interfacing hollow-core photonic bandgap fiber with atom trapping and atom interferometry experiments.

T9.3 Quantum logic scheme for state detection of molecular ions

Shiqian Ding, Huanqian Loh, Roland Hablutzel, Dzmitry Matsukevich

Thursday, February 27, 02.20 PM, Rooms 5+6

Quantum state detection of a single molecular ion can be applied towards precision measurement and controlled studies of cold chemistry. Such detection can be performed using quantum logic techniques, where the internal state of the molecular ion is mapped onto the state of a co-trapped atomic ion by coupling both of them to the common motional modes. The rotational state of the molecular ion can therefore be read out using the fluorescence of atomic ion. Further, we can use Zeeman splitting as a signature of different rotational levels due to their different magnetic g-factors. We will report implementation of this scheme using two atomic ions as a proof-of-principle experiment.

6.10 T10 Plasmonics and Metamaterials

This session will be held on Thursday, February 27, from 03.30 PM to 05.10 PM. Venue for this session is Rooms 1+2. Time allocated for invited talks is 25 min speaking time, plus 5 min Q&A, and time allocated for contributed talks is 15 min speaking time plus 5 minutes Q&A.

T10.1 High Q quadrupole and Fano resonances in THz metamaterials (INVITED)

Ranjan Singh, Wei Cao, Ibraheem Al-Naib, Weili Zhang

Thursday, February 27, 03.30 PM, Rooms 1+2

Losses in metamaterials arises from the Ohmic resistance of the materials used to fabricate the meta-atoms as well as the radiation resistance. Metals are the most widely used material for fabricating the meta-atoms such as split-ring resonators (SRRs) due to their high conductivity. At optical and near infrared frequencies, even the highest conducting metals exhibit Ohmic losses, thus requiring a new plasmonic material to be discovered in order to overcome the large resistive losses in optical plasmonic metamaterials. However, at far infrared frequencies, the most commonly used metals for metamaterials like silver, aluminum and gold have very high conductivity. The ultrahigh conductivity ensures much lower resistive losses at terahertz frequencies. In recent times, there have been several attempts to control the losses in SRRs by enhancing the metallic conductivities at cryogenic temperatures as well as by using superconductors. Though, these approaches succeeded in reducing the non-radiative losses to nearly zero but there has been no significant improvement in the quality factor (Q) of the metamaterial resonances due to the existing radiative loss channels in these planar resonators. The typical values of Q-factor in the terahertz, infrared and optical plasmonic metamaterials is less than 10. The Q-factor of any resonator is the measure of photon lifetime inside the structure. Higher Q-factor corresponds to longer lifetime and also determines the number of times a photon circumnavigates within the resonator. So far, it has been extremely difficult to achieve ultra-high Q-factors in planar metamaterial resonators due to excessive losses. In this talk, we report extremely high Q-factor quadrupole and Fano resonances in planar terahertz metamaterials by suppressing the radiative losses. The Q-factor values obtained is at least one order of magnitude higher than all the previous demonstrations and forms an ideal platform for high resolution ultrasensitive terahertz sensing.

T10.2 All-Polymer Distributed Bragg Reflectors

Paola Lova, Luca Boarino, Michele Laus, Franco Marabelli, Cesare Soci, Davide Comoretto

Thursday, February 27, 04.00 PM, Rooms 1+2

Polymeric Distributed Bragg Reflectors (DBRs) are 1D photonic crystals used in organic optoelectronic devices such as LEDs, lasers and sensors. They can be simply prepared by repeated spin coating of orthogonal polymer solutions, but usually suffer from poor refractive index contrast; moreover, availability of highly transparent materi-

als is rather limited.1 To overcome these limitations, the polymer refractive index can be modified using oxides and metal fillers, still preserving processability and transparency. Here we used ZnO:polystyrene (PS) nanocomposites to increase the refractive index of the PS matrix and employed it in a multilayer structure. The new material was produced by spin coating of PS-toluene solution, loaded with ZnO (n=1.98) nanoparticles that were synthetized by solvothermal route and grafted with a silane to reduce phase segregation in the non-polar matrix. Such procedure led to an increase of PS matrix refractive index (n=1.58) up to about 2

[1] L. Frezza, M. Patrini, M. Liscidini and D. Comoretto, J. Phys. Chem. B 115 (40), 19939 (2011)

T10.3 Plasmonic resonance: towards high efficiency terahertz absorber (INVITED)

Withawat Withayachumnankul

Thursday, February 27, 04.20 PM, Rooms 1+2

Plasmonics has recently become a very active topic in the rapidly growing area of nanophotonics. One unique aspect driving research activities in this direction is the sub-diffraction confinement of propagating waves along the interface between a conductor and dielectric, the so-called surface plasmon polaritons (SPPs). This aspect has led to a multitude of breakthroughs in sensing and imaging in recent years. At visible and UV frequency ranges, noble metals have their properties suitable to sustain SPPs. In contrast, at terahertz frequencies, metal properties approach a perfect electric conductor (PEC), leading to field delocalization into grazing waves. Periodically structured metal surfaces or moderately doped semiconductors can help to increase the terahertz wave confinement, leading to designer or spoof SPPs. This seminar discusses the properties of semiconductors suitable for terahertz plasmonic waves. Further, it focuses on microstructures that result in the resonance of SPPs, known as the localized surface plasmon resonance. Unique properties of these resonators are identified. A potential application in perfect absorbers will be discussed.

T10.4 Combinatorial Mapping Multipole Modes in Nanoclocks

Hailong Liu, Hongjin Fan, Nikolay Zheludev, Cesare Soci

Thursday, February 27, 04.50 PM, Rooms 1+2

We present a new platform, the plasmonic nanoclocks, for manipulating and engineering high-order plasmon modes with minimal change of design parameters. We experimentally establish the fundamental relations between the “time” displaying on the array of gold nanoscale clock dials and multipole plasmonic resonances. A combinatorial mapping of multipole modes of nanoclocks in analogy to the topologically equivalent movements of real-clock hands on a toroidal surface is presented.

6.11 T11 Nonlinear Optical Phenomena

This session will be held on Thursday, February 27, from 03.30 PM to 05.10 PM. Venue for this session is Rooms 3+4. Time allocated for invited talks is 25 min speaking time, plus 5 min Q&A, and time allocated for contributed talks is 15 min speaking time plus 5 minutes Q&A.

T11.1 Interpretation of Resonant Seeding Effect in Modulation Instability in Optical Fibers

Duc Minh Nguyen, Di Yang, Cesare Soci, Xuan Quyen Dinh, Ming Tang, Ping Perry Shum

Thursday, February 27, 03.30 PM, Rooms 3+4

We give a physical interpretation of the dynamics of resonant seed modulation instability of quasi-continuous pico-second pulses in terms of cascaded four-wave mixing and Bragg scattering in fiber frequency combs. We also report a critical condition to excite the resonant seeding effect.

T11.2 Highly efficient polarization entangled source for a loophole free bell test

Siddarth Koduru Joshi, Chen Ming Chia, Alessandro Cerè, Christian Kurtsiefer

Thursday, February 27, 03.50 PM, Rooms 3+4

Bipartite entanglement plays a crucial role in many quantum communication and computation protocols and fundamental tests of quantum mechanics (like a Bell test). Spontaneus Parametric Down Conversion (SPDC) allows the generation of pairs of photons with one or more degrees of freedom partially or completelly entangled.

We present a source of photons pairs with a tunable degree of polarization entanglement. The generated photon pairs are efficiently coupled into single mode fibers providing a high pairs to single ratio. A pump laser (wavelength = 405 nm)is focused into a type II PPKTP crystal, where it undergoes SPDC into signal and idler modes collinear with the pump mode. The bandwidth of the signal and idler photons is 128(4) GHz. The spectral brightness of the source is 14500 pairs/s/mW/nm.

To obtain a polarization entangled state, we pump the crystal from both directions and combine the two downconverted paths in a Sagnac interferometer. We control the degree of entanglement of the photon pairs by adjusting the power in each pump mode. The high fidelity (99.2

Many device-independent applications (such as cryptography, random number generation) and loophole free Bell tests require a source of entanglement which can produce states with a controllable degree of entanglement and a high pair to singles ratio. Although other high efficiency sources have been reported, they either have a lower efficiency, lower visibility or do not produce an entangled state [2–4]. Our pair source allows us to control the degree of entanglement while maintaining a high pairs to singles ratio and fidelity.

References 1. P.H. Eberhard, Background level and counter efficiencies required for a

loophole-free Einstein-Podolsky-Rosen experiment Phys Rev. A 47, R747 (1993) 2. B.G. Christensen, et al. Detection-Loophole-Free Test of Quantum Nonlocality, and Applications PRL 111, 130406 (2013). 3. M. Giustina,et al. Bell violation using entangled photons without the fair-sampling assumption Nature 497, 227230 (2013). 4. M. D. C. Pereira, et al. Demonstrating highly symmetric single-mode, single-photon heralding efficiency in spontaneous parametric downconversion Optics Letters, 38, 10, 1609-1611 (2013).

T11.3 Vortices in spinor cold exciton condensates with spin-orbit interaction

Helgi Sigurdsson, Timothy Liew, Oleksandr Kyriienko, Ivan Shelykh

Thursday, February 27, 04.10 PM, Rooms 3+4

We study theoretically the ground states of topological defects in a spinor four-component condensate of cold indirect excitons. We analyze possible ground state solutions for different configurations of vortices and half-vortices. We show that if only Rashba or Dreselhaus spin-orbit interaction (SOI) for electrons is present the stable states of topological defects can represent a cylindrically symmetric half-vortex or half vortex-antivortex pairs, or a non-trivial pattern with warped vortices. In the presence of both of Rashba and Dresselhaus SOI the ground state of a condensate represents a stripe phase and vortex type solutions become unstable.

T11.4 One-dimensional Van Hove polaritons

K. B. Arnardottir, O. Kyriienko, M.E. Portnoi, I.A. Shelykh

Thursday, February 27, 04.30 PM, Rooms 3+4

We studied the light-matter coupling of microcavity photons and an internband transition in a one-dimensional nanowire. Due to the Van Hove singularity in the density of states, resulting in a resonant character of the absorption line, the achievement of strong coupling becomes possible even without the formation of a bound state of an electron and a hole. The calculated absorption in the system and corresponding energy spectrum reveal anticrossing behavior characteristic of the formation of polariton modes. In contrast to the case of conventional exciton polaritons, the formation of 1D Van Hove polaritons will not be restricted to low temperatures and can be realized in any system with a singularity in the density of states.

T11.5 Chalcogenide Optical Axons and Photonic Synapses

Behrad Behrad, Paul Bastock, Khouler Khan, Chris Craig, Dan Hewak, Nikolay Zheludev, Cesare Soci

Thursday, February 27, 04.50 PM, Rooms 3+4

The cognitive functionality implemented within mammalian central neurons is the basis for the adaptable nature of our brains. Here, we demonstrate all-optical axons and synapses using sulphide fibers, capable of optically holding a neural resting state and generating and propagating photonic action potentials. Optical axons and photonic synapses created using this configuration, allow the realisation of various neuromophic concepts within a photonic platform including temporal and spatial summation, as well

as excitatory and inhibitory post synaptic potentials, culminating in the exhibition of short term and long term plasticity in an all-optical system. Furthermore, the use of fiber mass manufacturing technique utilised in the fabrication of these optical axons, makes them a low cost industrially friendly method to achieve a cognitive photonic platform.

6.12 T12 Atom-Photon Interaction

This session will be held on Thursday, February 27, from 03.30 PM to 04.50 PM. Venue for this session is Rooms 5+6. Time allocated for invited talks is 25 min speaking time, plus 5 min Q&A, and time allocated for contributed talks is 15 min speaking time plus 5 minutes Q&A.

T12.1 Two-stage magneto-optical trapping of 6Li using D2 line and narrow line UV cooling to reach high phase space density

Jimmy Sebastian, Christian Gross, Li Ke, G.H.C Jaren, Wenhui Li, Kai Dieckmann

Thursday, February 27, 03.30 PM, Rooms 5+6

Atoms at ultracold temperatures allow us to study many body quantum physics analogous to systems ranging from condensed matter to high-energy physics. Fermionic lithium is particularly suited to explore quantum many body physics in the strongly interacting regime. Recently there has been a great amount of interest to further cool atoms, such as potassium and lithium, where the unresolved hyperfine splitting of the excited state inhibits sub-Doppler cooling mechanisms. Apart from cooling atoms by sympathetic cooling using a second species [1], There are three ways to implement this. First is the use of grey molasses cooling, which is demonstrated in the case of 7Li [2], 40K [3] and 39K [4]. The second is the use of narrow line laser cooling where the narrow line width of the transition results in lower Doppler temperature as shown in the case of 40K [5] and 6Li [6]. In the third case Sisyphus cooling is done on the fine structure by detuning the laser far away compared to the hyperfine splitting as shown in the case of 7Li [7], but the 3D temperature obtained was much higher and the fraction of atoms cooled was lower than reported in [2] and [6]. We report here the cooling and trapping of neutral Fermionic 6Li atoms to high phase space density and low temperature. Usually 6Li is cooled and trapped using the broader D2 line, along the $2S_{1/2} \rightarrow 2P_{3/2}$ transition at 671 nm, which gives a Doppler temperature of 140 µK. The narrow-line $2S_{1/2} \rightarrow 3P_{3/2}$ transition at 323 nm results in a lower Doppler temperature of 18 µK. By loading precooled atoms in to the UV (323 nm) Magneto–optical trap (MOT) from the 671 nm MOT we are able to achieve a high phase space density of 4×10^{-4}, which is an order of magnitude higher than what is reported in [2] and [6]. By lowering the MOT beam intensities at the end of the UV MOT phase we are able to reach a mean 3D temperature of 33 µK, which is about 40

References: [1] M. Taglieber et al, Physical Review Letters, 100, 010401 (2008); [2] Andrew T. Grier et al, Physical Review A 87, 063411 (2013); [3] D. Rio Fernandes et al, EPL, 100, 63001 (2012); [4] G. Salomon et al, EPL, 104, 63002 (2014); [5] D. C. McKay et al, Physical Review A 84, 063420 (2011); [6] P. M. Duarte et al, 84, 061406, Physical Review A(R) (2011); [7] Paul Hamilton et al, arXiv:1308.1935.

T12.2 A Superradiant Laser

Zilong Chen, Justin Bohnet, Joshua Weiner, Dominic Meiser, Murray Holland, James Thompson

Thursday, February 27, 03.50 PM, Rooms 5+6

In this talk, I will present the experimental realization of a superradiant Raman laser. Steady-state collective emission, or superradiance, from ensembles of laser cooled atoms has been proposed as a method for generating sub-millihertz linewidth optical lasers, with potential for broad impacts across science and technology. We have built a model system that tests key predictions for such active oscillators using a laser cooled Raman laser operating deep in the bad-cavity, or good-gain-medium, regime of laser physics, where the cavity decay rate is much greater than the atomic coherence decay rate.

Specifically, we demonstrate that a system of 10^6 ^{87}Rb atomic dipoles cooled and tightly confined in an optical cavity can spontaneously synchronize and collectively emit a continuous coherent optical output, even when the intra-cavity field contains on average < 1 photon. By operating a low intra-cavity photon number, we demonstrate isolation of the collective atomic dipole from the environment by measuring a suppression of cavity frequency pulling by more than 10^4. The linewidth of the emitted light, measured relative to the Raman dressing laser, is less than the single-particle decoherence linewidths, demonstrating that the collective atomic coherence is more robust than single particle coherence. Our results verifies several key predictions for future superradiant lasers, which could be a frequency standard by itself, or be used to improve the stability of passive atomic clocks.

Reference: A steady-state superradiant laser with less than one intracavity photon, Nature 484, 78 (2012), doi: 10.1038/nature10920

T12.3 Counterintuitive temporal shape of single photons

Gurpreet Kaur Gulati, Bharath Srivathsan, Brenda Chng, Alessandro Cerè, Christian Kurtsiefer

Thursday, February 27, 04.10 PM, Rooms 5+6

We prepare heralded single photon states from a photon pair source based on nondegenerate four-wave mixing in an atomic vapour using a cascade level scheme [1]. These photons show anti-bunching with $g^{(2)}(0) < 0.03$, indicating a high single photon fidelity [2]. In an optical homodyne measurement we directly measure the temporal envelope of these photons inherited from the cascade decay. We observe an exponential decay for the idler photon (heralded on the signal) and counterintutively, an exponential rise for the signal photon (heralded on the idler). Furthermore, we show that by inverting the temporal profile of the herald photons with an asymmetric cavity, we obtain single photons of the desired wavelength and rising exponential temporal profile, ideal for efficient interaction with a single 87Rb atom [3, 4]. At the same time, our experiment illustrates the breakdown of a realistic interpretation of the heralding process in terms of defining an initial condition of a physical system [5].

References: [1] B. Srivathsan, et al. Narrow Band Source of Transform-Limited Photon Pairs via Four-Wave Mixing in a Cold Atomic Ensemble Phys. Rev. Lett. 111, 123602 (2013); [2] P. Grangier, et al. Experimental Evidence for a Photon Anticorrelation Effect on a Beam Splitter: A New Light on Single-Photon Interferences, Europhysics Letters 1, 4, 173 (1986); [3] M. Bader, et al. Efficient coupling to an optical resonator by exploiting

time-reversal symmetry New Journal of Physics 15, 12, 123008 (2013); [4] S. A. Aljunid, et al. Excitation of a single atom with exponentially rising light pulses Phys. Rev. Lett. 111, 103001 (2013); [5] Albert Einstein, et al. Can Quantum-Mechanical Description of Physical Reality Be Considered Complete? Phys. Rev. 47, 777 (1935).

T12.4 Towards Hong-Ou-Mandel Inteference of Single Photons from Four-Wave Mixing in an Atomic Ensemble and Spontaneous Emission from a Single Atom

Victor Xu Heng Leong, Sandoko Kosen, Gleb Maslennikov, Christian Kurtsiefer

Thursday, February 27, 04.30 PM, Rooms 5+6

Interference of photons emerging from different atomic systems is important for building practical quantum information networks. We report on the progress towards a Hong-Ou-Mandel interference experiment to test the indistinguishability of single photons produced via a four-wave mixing(FWM) process in a cold atomic ensemble of ^{87}Rb and spontaneous emission from a single ^{87}Rb atom in an optical dipole trap. The FWM process[1] uses a cascade decay scheme to generate pairs of time-correlated single photons of wavelengths 776 nm and 780 nm, while we generate single photons from a single atom by using a short π pulse to excite the atom to the $5P_{3/2}, F = 3, m_F = -3$ state and collecting the spontaneously emitted 780 nm photon. We aim to interfere the 780 nm photons from both systems on a 50:50 beamsplitter and observe the Hong-Ou-Mandel interference effect. These photons have comparable bandwidths but tuning with acousto-optical modulators is necessary to match their frequencies exactly.

[1] B Srivathsan et al., Phys. Rev. Lett. 111, 123602 (2013)

6.13 T13 Oxide Materials

This session will be held on Friday, February 28, from 09.00 AM to 10.40 AM. Venue for this session is auditorium. Time allocated for invited talks is 25 min speaking time, plus 5 min Q&A, and time allocated for contributed talks is 15 min speaking time plus 5 minutes Q&A.

T13.1 Electronic Reconstruction and Phase Emergence at the $LaAlO_3/SrTiO_3$ Interface (INVITED)

Alexander Petrovic

Friday, February 28, 09.00 AM, auditorium

Ten years after the discovery of a conducting channel at the $LaAlO_3/SrTiO_3$ interface, this fascinating heterostructure continues to generate controversy and surprises in equal measure. Chief among these is the apparent coexistence of superconductivity and ferromagnetism, which has proved particularly difficult to reconcile. We show that a hysteresis in the magnetotransport below the superconducting transition is a signature of vortex generation and depinning by discrete ferromagnetic dipoles, which are strictly confined to the interface above a narrow 2D superconducting channel. The ferromagnetism is present independently of the carrier density from 10^{13}–$10^{15}\,\mathrm{cm}^{-2}$ and experiences a competitive relationship with superconductivity. Examining the Shubnikov-de Haas oscillations which emerge at carrier densities above $6.9\times10^{14}\,\mathrm{cm}^{-2}$, we also demonstrate that the Fermi surface below the interface deviates from that of bulk $SrTiO_3$ over a distance of at least 120 nm, i.e. an order of magnitude greater than previously anticipated. We tentatively attribute this reconstruction to compressive strain from the $LaAlO_3$ layer.

T13.2 Science of Oxides for Electronics, Data Storage, Energy and Health (INVITED)

Thirumalai Venkatesan

Friday, February 28, 09.30 AM, auditorium

In this talk I will give a glimpse of the research ongoing at NanoCore in the science behind the use of oxides in various applications. Oxides, unlike their semiconducting or metallic counterparts are truly multi-faceted and one of the exceptional features of this system is the strong electronic correlation which introduces a number of unusual behavior.

I will illustrate some of these features with specific examples involving familiar oxide materials such as TiO2, VO2, and oxide interfaces. The bio-oxide interface seems to promise some exciting new frontiers for research and I will share some of our recent results in this area as well.

T13.3 Interface-Induced Magnetic Coupling in Multiferroic/Ferromagnetic Bilayer: An Ultrafast Pump-Probe Study

Chan La-O-Vorakiat, Y. Tian, Tom Wu, Christos Panagopoulos, Jian-Xin Zhu, Haibin Su, Elbert E. M. Chia

Friday, February 28, 10.00 AM, auditorium

By use of optical pump-probe measurement, we study the relaxation dynamics of a muliferroic-ferromagnetic $TbMnO_3/La_{0.7}Sr_{0.3}MnO_3$ bilayer. The relaxation dynamics of both layers are well separated in time allowing us to investigate the magnetic coupling across the bilayer. We observe that the relaxation dynamics of the individual layers in the bilayer sample are the result of the interplay between the intrinsic magnetic order and the induced interfacial effect. Our data suggest the existence of induced ferromagnetic order in the TbMnO3 layer, and antiferromagnetic order in the $La_{0.7}Sr_{0.3}MnO_3$ layer.

T13.4 Magnetic Control of the Optical Spin Hall Effect

Skender Morina, T. C. H. Liew, Ivan Shelykh

Friday, February 28, 10.20 AM, auditorium

A quantum microcavity is composed of a quantum well sandwiched between two Distributed Bragg Reflectors (DBR) which give the cavity a very high Q-factor. In the strong coupling regime of light and matter in microcavities, the elementary excitations of the system are the so-called exciton-polaritons, which have both photonic and excitonic properties. We investigate theoretically the effect of an external magnetic field on the polarization patterns appearing in quantum microcavities due to the optical spin Hall effect, resulting from an effective magnetic field the polaritons experience. We show, by numerical modelling, that an increase in the real magnetic field perpendicular to the plane of the cavity, resulting in the increase of the Zeeman splitting, leads to the transition from azimuthal separation of polarizations to their radial separation. This effect can be straightforwardly detected experimentally, by analyzing the polarization of the emitted light.

6.14 T14 Soft Condensed Matter

This session will be held on Friday, February 28, from 09.00 AM to 10.30 AM. Venue for this session is Rooms 1+2. Time allocated for invited talks is 25 min speaking time, plus 5 min Q&A, and time allocated for contributed talks is 15 min speaking time plus 5 minutes Q&A.

T14.1 Elasticity of Compressed Microgel Suspensions (INVITED)

Massimo Pica Ciamarra, Giovanni Romeo

Friday, February 28, 09.00 AM, Rooms 1+2

The elastic properties of crystals are rationalized exploiting the periodicity of their lattice structure, that allows for the developing of a tractable solution of a system of masses connected by springs. Indeed, the absence of periodicity makes a challenge the understanding of the elastic properties of amorphous solids. When dealing with soft materials, i.e. solids whose "atoms" are macroscopic objects, this problem could be even more complicated as particles might shrink or deform. Here we show that it is actually possible to describe the elasticity of compressed microgel suspensions starting from a core–shell model for the single particle, i.e. that it is possible to connect the macroscopic scale with the sub-particle scale. The mechanical properties of the inner core and of the outer corona are described via the mean field Flory theory, and via the Alexander–de Gennes model for polymer brushes, respectively. The model successfully reproduces experimental measures of the elastic shear modulus up to a constant factor that we rationalize in the jamming perspective.

T14.2 Size and density avalanche scaling near jamming

Roberto Arevalo, Massimo Pica Ciamarra

Friday, February 28, 09.30 AM, Rooms 1+2

The current microscopic picture of plasticity in amorphous materials assumes local failure events to produce displacement fields complying with linear elasticity. Indeed, the flow properties of nonaffine systems such as foams, emulsions and granular materials close to jamming, that produce a fluctuating displacement field when failing, are still controversial. Here we show, via a thorough numerical investigation of jammed materials, that nonaffinity induces a critical scaling of the flow properties dictated by the distance to the jamming point. We rationalize this critical behavior introducing a new universal jamming exponent and hyperscaling relations, and use these results to describe the volume fraction dependence of the friction coefficient.

T14.3 Axisymmetric pulsating flow within a thin gap

Milad Mohammadzadeh, Fenfang Li, Claus-Dieter Ohl

Friday, February 28, 09.50 AM, Rooms 1+2

Driven by the need to rapidly stretch cells we utilize a laser-induced rapidly expanding vapor bubble in a microfluidic channel. Cells near the bubble become strongly elongated which allowed us to obtain an upper limit to the critical yield strength of red blood cells

[1]. In this work, we focus on understanding the flow field generated by the explosively expanding bubble. This fluid mechanics problem has some resemblance to the classical yet unsolved axisymmetric flow created by a time varying source/sink in a thin gap. We conduct numerical simulations using a commercial flow solver (Ansys Fluent) based on volume-of-fluid (VOF) method which utilizes a multiphase model and accounts for viscosity and surface tension. The flow created by the expanding and shrinking bubble leads to boundary layer separation, recirculation, and very strong shear near the walls. The basic mechanism is the adverse pressure gradient at the onset of bubble shrinkage. Although the solution is rather complex, its main features can be obtained by simplifying assumptions for which analytical solutions exists. We thus compare the CFD and the analytical solutions and explain why red blood cells are stretched through this flow but larger cells are not.

[1] Li, F., Chan, C. U., & Ohl, C. D. (2013). Yield Strength of Human Erythrocyte Membranes to Impulsive Stretching. Biophysical journal, 105(4), 872-879.

T14.4 Cleaning with acoustic cavitation bubbles in water supersaturated with air

Tatsuya Yamashita, Keita Ando

Friday, February 28, 10.10 AM, Rooms 1+2

Ultrasonic cleaning in water several hundred percent supersaturated with air is observed to compare the cleaning effect with usual tap water. The supersaturated water is generated with Venturi aeration method in which the fission of micro-sized bubbles floating in circulating water flow is induced by the pressure recovery at the diverging outlet; the resulting bubble size is submicron so that bubble dissolution rate is expected to increase. The sufficient level of supersaturation with air is shown to create micro-sized gas bubbles on glass surfaces and they act as cleaning agents, which oscillate under 65 kHz focused acoustic irradiation (2s duration). Their dynamics is observed using a high-speed camera and dissolved oxygen is measured before each irradiation. The cleaning effect does not depend on the level of dissolved oxygen but on the pre-existing bubble size. The most notable particle removal is observed when pre-existing bubble radiuses are near the resonant size based on ultrasonic frequency. Once these bubbles grow beyond the resonant size, their cleaning effect disappears. This suggests a possibility to achieve the optimum cleaning timing following the pre-existing bubble size.

6.15 T15 Ultrafast Spectroscopy

This session will be held on Friday, February 28, from 09.00 AM to 10.30 AM. Venue for this session is Rooms 3+4. Time allocated for invited talks is 25 min speaking time, plus 5 min Q&A, and time allocated for contributed talks is 15 min speaking time plus 5 minutes Q&A.

T15.1 Long-range diffusion induced ultrafast and efficient charge carrier extraction in organic-Inorganic $CH_3NH_3PbI_3$ heterojunctions (INVITED)

Guichuan Xing, Swee Sien Lim, Tze Chien Sum

Friday, February 28, 09.00 AM, Rooms 3+4

Low-temperature solution-processed photovoltaics suffer from low efficiencies because of poor exciton or electron-hole diffusion lengths (typically about 10 nanometers). Recent reports of highly efficient $CH_3NH_3PbI_3$-based solar cells in a broad range of configurations raise a compelling case for understanding the fundamental photophysical mechanisms in these materials. By applying femtosecond transient optical spectroscopy to bilayers that interface this perovskite with either selective-electron or selective-hole extraction materials, we have uncovered concrete evidence of balanced long-range electron-hole diffusion lengths of at least 100 nanometers in solution-processed $CH_3NH_3PbI_3$. The high photoconversion efficiencies of these systems stem from the comparable optical absorption length and charge-carrier diffusion lengths, transcending the traditional constraints of solution-processed semiconductors.

T15.2 Singlet fission in organic crystals: femtosecond spectroscopy

Lin Ma, Christian Kloc, Cesare Soci, Handong Sun, Maria-Elisabeth Michel-Beyerle, Gagik Gurzadyan

Friday, February 28, 09.30 AM, Rooms 3+4

The excited state dynamics in organic crystals of rubrene and alpha-perylene were studied by use of ultrafast optical spectroscopy. Different decay channels such as singlet fission, energy trapping, polaron generation as well as excimer formation were investigated. Among them, singlet fission plays an important role in the excited state relaxations of both crystals and was studied in detail under both one- and two-photon/quantum excitation. Moreover, temperature-dependent fluorescence study reveals the interplay between singlet fission and the energy trapping process in rubrene. The discrepancy between the steady state absorption and fluorescence excitation spectra indicates there is a strong competition between singlet fission, dimer cation generation and excimer formation in alpha-perylene crystal.

T15.3 Ultrafast charge photogeneration in low band-gap semiconducting polymer based solid-state dye sensitized solar cell

Sai Santosh Kumar Raavi, Giulia Grancini, Jun Yin, Annamaria Petrozza, Henry Snaith, Cesare Soci, Guglielmo Lanzani

Friday, February 28, 09.50 AM, Rooms 3+4

Lately, there is a hot pursuit on the utility of conjugated polymers as hole transporting materials (HTM) in solid-state dye-sensitized solar cells (sDSC) due to their thermal stability, high conductivity, good solubility as well as tunable optoelectronic properties. In this work, we investigate the photo-induced charge generation in a high performance solid state dye sensitized solar cell with an indoline-based dye (D131) sensitizing mesoporous TiO_2 electrode and a low band gap polymer poly[2,6-(4,4-bis-(2-ethylhexyl) - 4Hcyclopenta[2,1-b;3,4-b]dithiophene)-alt- 4,7-(2,1,3-benzothiadiazole)] (PCPDTBT) (Eg$\approx$ 1.45 eV) as HTM. We combined a systematic experimental investigation from both photo-physics and device-point of view as well as a comprehensive density functional theory (DFT) calculations to understand the nature of photo-induced processes contributing towards enhanced photo-current. The photo-conversion efficiency of these devices measured under AM 1.5G simulated sun light were obtained to be $\approx$ 3.2%. In particular, we observe the contribution of photocurrent from the region of ground state absorption of the polymer from the external quantum efficiency measurement. Femtosecond transient absorption (TA) experiments were performed to obtain a clear picture of the role of polymer on the enhancement of overall photo-charge generation in the device configuration by following photo-processes occurring in the dye/polymer and dye/TiO2 interfaces by selectively exciting the dye (at 390 nm) and the polymer (at 780 nm). Exciting the dye/TiO_2 interface we observed ultrafast charge-generation in the order of $<$ 300 fs followed by low recombination kinetics suggesting the polymer as a good hole-transport material while exciting the polymer/dye interface we obtained long-lived charge dynamics in the spectral region of probe where the hole on the polymer absorbs thus confirming the role of polymer as a light harvesting antenna. Furthermore, the DFT calculations for the dimer system of polymer/dye suggest a strong electronic coupling between HOMOs of D131 and PCPDTBT which facilitates easy hole transfer from D131 to PCPDTBT; on the other hand, the appearance of two charge transfer (CT) states slightly below the bright $\pi^- > \pi^*$ state of D131 proves charge transfer from the dimer system to TiO2 thus confirming our experimental observation of ultrafast charge-generation and well as enhanced photovoltaic efficiency.

T15.4 Polaron Photogeneration in Polymer Bulk Heterojunctions: Influence of Film Morphology

Majid Panahandeh-Fard, Zilong Wang, Jun Yin, Manoj Kumar, Cesare Soci

Friday, February 28, 10.10 AM, Rooms 3+4

Morphology of the large-area interpenetrating network of donor and acceptor at the nanometer-scale has a strong influence on the performance of bulk heterojunction solar cells (BHJSCs). Morphological properties of the active layer film can be controlled by synthesis and processing methods to control charge photogeneration yield, and ultimately improve efficiency of BHJSCs. The optimal morphology requires a balance between large interfacial area of donor and acceptor domain size to facilitate exciton diffusion and dissociation, and continuous percolated pathways to the electrodes for charge carrier collection. Thermal annealing and process annealing by solvent additives have proven to greatly improve photovoltaic power conversion efficiency in typical

donor-acceptor systems like poly(3,4-dihexyloxythiophene) P3HT and fullerene derivative PC60BM. This is reflected by the yield and spectral signatures of photogenerated polarons probed by the Infra-Red Active Vibrational (IRAV) modes as well as visible-to near-infrared polaron peaks in steady state and transient photoinduced absorption spectra. Experiments correlating bulk heterojunction film morphology with charge carrier photogeneration yield and dynamics and to photovoltaic efficiency of devices will be presented.

6.16 T16 Quantum Sensing

This session will be held on Friday, February 28, from 09.00 AM to 10.20 AM. Venue for this session is Rooms 5+6. Time allocated for invited talks is 25 min speaking time, plus 5 min Q&A, and time allocated for contributed talks is 15 min speaking time plus 5 minutes Q&A.

T16.1 Quantum metrology with photonic polarization gears (INVITED)

Leong-Chuan Kwek

Friday, February 28, 09.00 AM, Rooms 5+6

Quantum metrology bears a great promise in enhancing measurement precision. Recently, we demonstrate that NOON-like photonic states using angular momentum states could be set up with a 'photonic gear' based on a 'super-resolving' Malus' law. We show that this effect leads to single-photon angular measurements with the same precision of polarization- only quantum strategies with m photons, but robust to photon losses. In our recent study, we also combine the gear effect with the quantum enhancement due to entanglement, thus exploiting the advantages of both approaches. The high 'gear ratio' m boosts the current state of the art of optical non-contact angular measurements by almost two orders of magnitude.

T16.2 Measuring Solar Photon Bunching (INVITED)

Peng Kian Tan

Friday, February 28, 09.30 AM, Rooms 5+6

In 1956, Hanbury-Brown and Twiss demonstrated that at sufficiently short timescales, both spatial and temporal correlation measurements of thermal light sources such as stars should exhibit a photon bunching signal that peaks at twice the statistically random noise floor. Recently there has been a revival of interest in repeating the Hanbury-Brown–Twiss method to map the spatial structure of stellar formations, detect earth sized planets and test various models of quantum gravity. However, due to the mismatch between the photon coherence time with detector resolution the thermal photon bunching signal is very weak and therefore difficult to distinguish from the dominant Poissonian noise with usual detection techniques . Optical spectral filtering may significantly improve the photon bunching Signal-to-Noise Ratio. We demonstrate this technique by explicitly resolving the photon bunching signal from the Sun.

T16.3 Adsorbate Electric Fields on a Cryogenic Atom Chip

Kin Sung Chan, Christoph Hufnagel, Rainer Dumke

Friday, February 28, 10.00 AM, Rooms 5+6

We investigate the behavior of electric fields originating from adsorbates deposited on a cryogenic atom chip as it is cooled from room temperature to cryogenic temperature. Using Rydberg electromagnetically induced transparency, we measure the field strength versus distance from a 1 mm square of yttrium barium copper oxide (YBCO) patterned onto a yttria stabilized zirconia chip substrate. We find a localized and stable dipole

field at room temperature and attribute it to a saturated layer of chemically adsorbed rubidium atoms on the YBCO. As the chip is cooled towards 83 K we observe a change in sign of the electric field as well as a transition from a localized to a delocalized dipole density. We relate these changes to the onset of physisorption on the chip surface when the van der Waals attraction overcomes the thermal desorption mechanisms. Our findings suggest that through careful selection of substrate materials, it may be possible to reduce the electric fields caused by atomic adsorption on chips, opening up experiments to controlled Rydberg-surface coupling schemes.

6.17 T17 Materials for Energy Conversion

This session will be held on Friday, February 28, from 11.00 AM to 12.30 PM. Venue for this session is auditorium. Time allocated for invited talks is 25 min speaking time, plus 5 min Q&A, and time allocated for contributed talks is 15 min speaking time plus 5 minutes Q&A.

T17.1 Novel oxygen reduction reaction (ORR) catalysts for PEM fuel cells (INVITED)

Jianyi Lin, Linfei Lai, Jilei Liu

Friday, February 28, 11.00 AM, auditorium

Polymer electrolyte membrane fuel cell (PEMFC) is a very promising energy conversion device with high efficiency, scalability and low carbon emission. Platinum supported on carbon is the only viable catalyst used for PEMFC today. The cost and stability of platinum catalysts are the barriers in wide-spread applications of PEMFC. Thus, the development of low loading Pt catalysts or low cost non-noble-metal catalysts (NNM) is highly desirable, especially at the cathode, where the oxygen reduction reaction (ORR) requires much higher Pt loading as compared to the anode. Various NNM catalysts for ORR have been studied in our labs, including N-containing graphene supported NNM and metal-carbide assisted low-loading Pt catalysts. N-doping was found to be crucially important in improving the ORR catalysts performance. Nitrogen-doped graphene was a better metal-free catalyst than pristine graphene for ORR due to the enhanced electron density in the catalyst valence band region. Non-noble metal catalysts such as transition-metal nitrides or carbides supported on N-doped graphene showed a performance compatible to commercial Pt catalysts for ORR, much better than the same transition metals supported on conventional carbon carriers such as graphite and activated carbon. SEM, XRD, XPS, UPS and electrochemical evaluations were employed to understand the reaction mechanism and the nature of the active centers.

T17.2 Sulfur based solid electrolytes for Lithium sulfur batteries

Rayavarapu Prasada Rao, Stefan Adams

Friday, February 28, 11.30 AM, auditorium

Rechargeable all-solid-state lithium- or Li-ion batteries are attractive power sources for small scale applications ('smart' credit cards, medical implants), but in the near future could also become relevant as bulk systems for a wider range of applications, as they improve safety and stability over conventional batteries with flammable liquid electrolytes. This requires electrochemically stable Li^+ fast ion conductors (FIC) as the solid electrolyte. Finding such stable fast ion conductors is thus the key to building practical solid-state batteries. There have been numerous developments on materials such as lithium rich sulfide glasses as solid electrolyte. However, low current density remains a major obstacle in these electrolyte systems. Among the most promising compounds with high ionic conductivities are the thiophosphate-based solid electrolytes. Our studies showed that disorder in the immobile sublattice is a crucial factor for maximizing their

conductivity. This is shown both for the argyrodite-type halide-doped thiophosphates Li_6PS_5X (where anion-ordered Li_6PS_5I exhibits the lowest ionic conductivity despite the lattice expansion by the large soft I-, while the S2-/X- disorder for X = Cl, Br opens up local paths for Li^+ motion) as well as for $Li_{10}(Ge,P)PS_{12}$, where the local P/Ge disorder limits the packing density and leaves free volume for fast ion transport channels Li(1)-Li(3)-Li(3)-Li(1) along c and especially their interconnection to an anisotropic 3D pathway network via interstitial Li(4) sites. The nearly ideal hopping distance of 1.7 - 2.3 Å among partially occupied sites and the moderate energy required for interconnections between the 1D channels render this structure type particularly suited to combine fast ion transport with structural stability. The only fully occupied Li site, Li(2), does not participate in ion transport and its isomorphous replacement could further optimize the properties of this novel class of solid electrolytes. In situ neutron powder diffraction of ball milled precursors showed that a crystalline argyrodite phase, essentially Li_7PS_6, forms from extensively ball-milled precursors with the Li_6PS_5Cl stoichiometry at temperatures as low as 80°C, but it takes significantly higher annealing temperatures (>430°C) and preferentially fast cooling to reach the composition Li_6PS_5Cl. This explains why samples crystallized at low temperatures such as 150 °C do not exhibit the same fast-ionic conductivity as those crystallized at higher temperatures. Our electrochemical impedance studies showed the ionic conductivity of Li_6PS_5Cl is 0.7 mS/cm and $Li_{10}GePS_{12}$ is 1.68 mS/cm at room temperature. All solid state battery using $Li_4Ti_5O_{12}$/ Li_6PS_5Cl/Li showed a first discharge capacity, ≈75 mAh/g, with 99% columbic efficiency. S/$Li_{10}GeP_2S_{12}$/In-Li battery with current density 70 mA/g showed an initial discharge capacity of 685 mAh/g.

T17.3 Pyridine-Capped InP Quantum Dots as Electron Acceptors for Polymer Photovoltaics

Jun Yin, Manoj Kumar, Qiong Lei, Majid Panahandeh-Fard, Daniele Cortecchia, Zilong Wang, Sai Santosh Kumar Raavi, Cesare Soci

Friday, February 28, 11.50 AM, auditorium

Indium phosphide (InP) quantum dots (QDs) have attracted a great deal of attention because of their excellent electronic properties and widely size-tunable emission in the visible range, as well as improved performance for applications in hybrid organic/inorganic solar cells. The interfacial energy mismatch between InP and low-bandgap polymers like P3HT is ideal to form type-II hybrid heterojunctions and promote charge separation. However, organic ligands used to stabilize the QD suspensions often increase their LUMO energy, with detrimental effects on photovoltaic efficiency. In this work we combine density functional theory (DFT) with femtosecond transient absorption spectroscopy to characterize the effects of organic ligands on charge carrier photogeneration and transfer dynamics in a hybrid P3HT/InP QDs system. DFT predictions show that the LUMO energy of the QDs increases proportionally to the surface coverage, but this undesirable effect can somehow be mitigated when using short conjugated ligands, such as pyridine, that lower the QD HOMO-LUMO gap, increasing spectral overlap with solar irradiance. Meanwhile, the substitution of the original oleylamine stabilizing

ligands with a pyridine capping layer with lower surface coverage can promote electron localization to the core of the InP QDs and hole delocalization over the pyridine ligands. We also observe notable quenching of the photoluminescence intensity of InP/P3HT thin films compared to pure P3HT and InP QD films, an indication of efficient photoinduced charge transfer across the InP/P3HT heterointerface. Photoinduced absorption measurements confirm ultrafast ($t < 260\,\mathrm{fs}$) formation of polarons and subsequent (t<1 ps) electron injection into the InP QDs, and enhancement of the polaron formation yield. Fast electron injection into the InP QD acceptors is in good agreement with the strong coupling ($\approx 15.4\,\mathrm{meV}$) between the lowest unoccupied molecular orbitals of P3HT and QDs in the ground state predicted by DFT. This suggests that the use of different organic molecules, especially short conjugated ligands, for InP QDs passivation may be used to control the charge carrier wavefunctions, providing a tuneable parameter in the design of QDs-based functional composites for photovoltaic applications.

T17.4 A Facile Laser Modification of ZnO/CdSSe Core/Shell Nanowire Arrays with Improved Optical Properties en Route to Advanced Functionality

Junpeng Lu, Chorng Haur Sow

Friday, February 28, 12.10 PM, auditorium

Arrays of ZnO/CdSSe core/shell nanowires with shells of tunable band gaps have been synthesized via a simple chemical vapor deposition approach. On the basis of their type II heterojuntions and chemical compositions, these nanowire arrays give out unique photoelectrical properties. In this work, we demonstrate that a direct focused laser beam irradiation was able to achieve localized modification of the hybrid structure and chemical composition of the nanowire arrays. As a result, we could locally improve the optical properties of these arrays. With a scanning laser beam, micropatterns with different fluorescence emissions could be created on a substrate covered with nanowire arrays. This could realize the encryption application via carefully controlling the laser power. A 3D photodetector with superior performance has been demonstrated using laser modified nanowire arrays assembled with monolayer graphene as the electrode.

6.18 T18 Physics of Batteries

This session will be held on Friday, February 28, from 11.00 AM to 12.20 PM. Venue for this session is Rooms 1+2. Time allocated for invited talks is 25 min speaking time, plus 5 min Q&A, and time allocated for contributed talks is 15 min speaking time plus 5 minutes Q&A.

T18.1 Three-Dimensional Graphene Foam Supported Fe_3O_4 Lithium Battery Anodes with Long Cycle Life and High Rate Capability

Jingshan Luo, Jilei Liu, Jianyi Lin, Zexiang Shen, Hongjin Fan

Friday, February 28, 11.00 AM, Rooms 1+2

Fe_3O_4 has long been regarded as a promising anode material for lithium ion battery due to its high theoretical capacity, earth abundance, low cost and nontoxic properties. However, up to now, no effective and scalable method has been realized to overcome the bottleneck of poor cyclability and low rate capability. In this article, we report a bottom up strategy assisted by atomic layer deposition (ALD) to graft bicontinuous mesoporous nanostructure Fe_3O_4 onto three dimensional (3D) graphene foams and directly use the composite as the lithium ion battery anode. This electrode exhibits high reversible capacity and fast charging and discharging capability. A high capacity of 785 mAh/g is achieved at 1C rate and is maintained without decay up to 500 cycles. Moreover, the rate of up to 60 °C is also demonstrated, rendering a fast discharge potential. To our knowledge, this is the best reported rate performance for Fe_3O_4 in lithium ion battery to date.

T18.2 Atomic-Layer-Deposition-Assisted Formation of Carbon Nanoflakes on Metal Oxides and Energy Storage Application

Cao Guan, Hongjin Fan

Friday, February 28, 11.20 AM, Rooms 1+2

Nanostructured carbon is widely used in energy storage devices (e.g., Li-ion and Li-air batteries and supercapacitors). We will present our discovery of a new method towards the generation of carbon nanoflakes on nearly any type of solid substrates by combining atomic layer deposition (ALD) and carbonization process. Using various metal oxide nanostructures as the example, metal oxide@nanoflake carbon (MO@f-C) core-shell nanostructures are obtained. The mechanism of the formation process is proposed as follows: the ALD Al2O3 and glucose form a composite layer during the soaking, which expands during thermal annealing, and nanoflake carbon deposits on the alumina skeletons, a phenomenon similar to 'coke' formation in catalyst. The obtained MO@f-C nanostructures were tested as electrochemical supercapacitor and lithium ion battery electrodes, which are to exhibit better performance compared with the pristine metal oxides or the carbon coating without ALD. For example, when tested as supercapacitor electrode, 1D CoO nanowire@f-C shows 2 times of capacitance than that of CoO alone. 2D NixCo1-xO nanowalls@f-C also show higher lithium storage capacity and improved cycling stability. The enhancement is largely due to the increased specific surface ar-

eas and increased electric conductivity. This peculiar carbon coating method with the unique hierarchical nanostructure may provide a new insight into the preparation of 'oxides + carbon' hybrid electrode materials for energy storage applications.

T18.3 (Ni1-xZnx)Fe2O4 SPINEL OXIDES AS HIGH PERFORMANCE ANODE MATERIALS FOR Li-ION BATTERIES

Chu Yao Quan, Keefe Wayne Teo, Lim Ji Ho, M. V. Reddy

Friday, February 28, 11.40 AM, Rooms 1+2

We prepared new solid solutions based on Ni, Zn and Fe-oxides as nano-materials for anodes of Li-ion batteries. The materials were synthesized using molten salt method with KCl as the eutectic salt. The molten salt method (MSM) is chosen as the preparation method as it is a simple and versatile method. Furthermore, it is a cheap method that can produce the desired compounds in bulk. The prepared nano-materials $Ni_{1-x}Zn_xFe_2O_4$ were characterized by Scanning Electron Microscopes (SEM), X-Ray Diffraction (XRD), the Brunauer-Emmett-Teller surface and density methods. Cyclic Voltammetry (CV) and Galvanostatic Cycling tests were also conducted to understand energy storage performance of the electrodes. Electrochemical impedance spectroscopy (EIS) was performed to analyse electrode kinetics and other characteristics of the cell. The electrochemical properties of prepared compounds showed a reversible capacity (mAh/g) of 706, 819, 536, 781, 637 for $x = 0, 0.25, 0.5, 0.75$ and 1 at the end of the 50th cycle. Not only our present values are higher than the theoretical capacity of commercial graphite ($372\,\mathrm{mAhg^{-1}}$), they possess better capacity retention, which makes them appropriate choices for anode materials.

T18.4 Nanostructured Metal oxides and Nitrides as Electrode Materials for Lithium Ion Batteries

M V Reddy Reddy, B V R Chowdari

Friday, February 28, 12.00 PM, Rooms 1+2

In my presentation, I will discuss the advantages of nanostructured morphology and different crystal structure, surface area on Li-storage properties. Few select ternary spinel oxides AB2O4 (A= Zn, Mn, Ni, Mg, B= Co, Fe) prepared by molten salt method, characterized by variety of techniques and cycled in the voltage range of 0.005-3.0V at a current rate of 60 mA/g will be discussed. Co_3O_4 showed a reversible capacity in the 830-950 mAhg-1 range at the end of 30th cycle and 0 to 12

References

[1] M.V. Reddy*, G.V. Subba Rao, B.V. R. Chowdari* "Metal oxides and oxysalts as anode materials for lithium ion batteries" Chemical Reviews 113(2013)5364-5457 (I.F.: 41.297, ACS (Highest impact factor Journal and for the 1st time an Asian university published critical review paper in highly ranked journal Chem. Rev. in the area of Li-batteries and this paper is one of top 4 highly read paper in Chemical Reviews Q2); [2] B. Das, M. V. Reddy, B. V. R. Chowdari NanoScale 5 (2013) 1961-1966; [3] M.V. Reddy*, Cai Yu, Fan Jiahuan, K.P. Loh, B.V.R. Chowdari ACS Applied Materials and Interfaces

5(10)(2013) 4361-4366; [4] M.V. Reddy*, Cai Yu, Fan Jiahuan, K.P.Loh, B.V.R. Chowdari RSC Advances 2(2012)9619-9625; [5] M.V. Reddy*, G. Prithivi, K.P.Loh, B.V.R. Chowdari ACS Applied Materials and Interfaces 6(1) (2014)680-690.

6.19 T19 Special Topics

This session will be held on Friday, February 28, from 11.00 AM to 12.20 PM. Venue for this session is Rooms 3+4. Time allocated for invited talks is 25 min speaking time, plus 5 min Q&A, and time allocated for contributed talks is 15 min speaking time plus 5 minutes Q&A.

T19.1 Cooperative dynamics in coupled socio-ecological system: the effect of network structure (INVITED)

Lock Yue Chew, Ning Ning Chung, Choy Heng Lai

Friday, February 28, 11.00 AM, Rooms 3+4

Darwin's theory of evolution based on survival of the fittest suggests selfish competition to be the modus operandi between individuals who aim to attain the highest benefit for themselves at the expense of others. However, counterintuitive to this notion, we witness the phenomenon of cooperative collaborations within many levels of social and biological organization. For example, we observe genes functioning in unison within genomes and hunters working in groups to gather food. In order to understand the omnipresence of such cooperative behaviour, various mechanisms have been proposed to elucidate how cooperation can arise out of the tenets of natural selection. Indeed, one hypothesis is to abandon the assumption of well-mixed population (i.e. everyone interacts with everyone else) and assumes that each individual only interacts with agents in its neighbourhood. Within the context of such a social network, several studies have reported that cooperative behaviour survives better when the average number of social ties is smaller.

While models of cooperative behaviour in social systems are well established, the quantitative investigation of cooperation within social and ecological systems that are coupled together has just begun. In fact, the study of cooperation in such coupled socio-ecological system has gained impetus rather recently in consequence of the inadvertent actions of human beings such as large-scale fishing and inconsiderate fresh water use that have left many Earth ecosystems devastated. An understanding on how cooperation can emerge in the form of social restraint in the use of natural resources to ensure sustainability is essential to curtail the continuous harm that is currently made to the Earth's environmental as well as ecological systems. Recently, S. Levin et. al. has introduced a model to study the establishment of cooperative behaviour in coupled socio-ecological systems through the social rule of ostracism against defectors who overuse the common pool resources. In this model, the population is assumed to be well-mixed. In this talk, I will show our extension of this model to populations with complex interaction patterns. In particular, we have modeled the interaction of individuals with their neighbours based on the approach of a complex network of social interactions. In contrast to studies on emergence of cooperation in social networks, both our numerical and analytical results have shown that cooperative behaviour in the use of common pool resources can be easily induced by social ostracism in a population where virtually everyone knows everyone else. On the other hand, social ostracism is found to be less effective in the promotion of cooperative behaviour in populations that possess fewer connections with each other. In

fact, we found that the formation of community within a population is not necessarily associated with a higher level of cooperation. In this respect, our results provide deeper insights into the manner in which governance structures can have important influence on the management of coupled socioecological systems.

T19.2 Measurement of Photon Statistics with Live Photoreceptor Cells (INVITED)

Leonid Krivitsky

Friday, February 28, 11.30 AM, Rooms 3+4

Interfacing biological objects with quantum light allows to enhance the precision of biological measurements, fosters development of models of biological processes, and allows to reveal possible role of quantum effects in neurobiology and perception. Rod cells of the retina are natural photodetectors, and they are perfect candidates for studies of biological interfaces with quantum light. We interface rod cells with light sources of different photon statistics [1, 2]. We show that similar to man-made photodetectors, the rod cells are able to discriminate between thermal and coherent statistics of light [1]. We also interface rod cells with a heralded single photon source [2]. This approach allows us to directly demonstrate single photon sensitivity of rod cells, to measure their quantum efficiency and assess parameters of single photon responses. The results are relevant to ongoing studies of manifestation of quantum effects in phototransduction, vision, and photosynthesis.

[1] N. Sim et al., Measurement of Photon Statistics with Live Photoreceptor Cells, Phys. Rev. Lett. 109, 113601 (2012) (Editor's suggestion). [2] N. M. Phan et al., Controllable stimulation of retinal rod cells using single photons, arXiv:1308.0670

T19.3 PDMS BASED Photoacoustic lens For Acoustic Holography

Yuanxiang Yang, Chenjie Xu, Claus-Dieter Ohl

Friday, February 28, 12.00 PM, Rooms 3+4

Concave optical lenses coated with a photoacoustic material and illuminated with an intense laser pulse allow the generation of high pressure transients in liquids. The lens surface acts as constant phase surface from which a single acoustical transient is launched through the conversion of light into pressure. More complex focusing such as Bessel beams and multiple spatial or temporal foci may be achieved with suitably shaped photoacoustic lenses. Here we show that with simple lab tools, complex acoustic emitters resembling transmission holograms can be generated. To achieve this we make the lens out of cured polydimethylsiloxane (PDMS). PDMS has excellent optical properties for the utilized wavelength of 532 nm and it is coated with black nail polish that acts as a photoacoustic material. The lens is molded from plastic which is printed with a low-cost 3D printer. We demonstrate PDMS based lenses focusing of single and multiple waves in water. For the latter a modified plano-concave lens with two staggered concave faces but identical focal point was fabricated and tested. These studies aim to develop a simple acoustic source for shock wave based ultrasound therapy.

7 Committees

Program Committee

KOH Wee Shing, IHPC, A*STAR

Cesare SOCI, SPMS, NTU

CHEN Xiadong, School of Materials Science and Engineering, NTU

Christian KURTSIEFER, CQT and Physics Dept, NUS

Organizing Committee

KOH Wee Shing, IHPC, A*STAR

Cesare SOCI, SPMS, NTU

Andreas DEWANTO, Faculty of Science, NUS

LIM Kim Yong, Faculty of Science, NUS

Evon TAN, CQT, NUS

special thanks for logistics help to Brenda CHNG, Victor LEONG, Gurpreet GULATI, Wilson CHIN and others from CQT, NUS, and the Utown management team

Christian KURTSIEFER, CQT and Physics Dept, NUS

Author List